

Liouville Theory and the Weil–Petersson Geometry of Moduli Space

Sarah M. Harrison,^{a,b} Alexander Maloney,^a and Tokiro Numasawa^c

^a*Department of Physics, McGill University, Montreal, QC, Canada*

^b*Department of Mathematics and Statistics, McGill University, Montreal, QC, Canada*

^c*Institute for Solid State Physics, University of Tokyo, Kashiwa 277-8581, Japan*

E-mail: sarah.harrison@mcgill.ca, alex.maloney@mcgill.ca,
numasawa@issp.u-tokyo.ac.jp

ABSTRACT: Liouville theory describes the dynamics of surfaces with constant negative curvature and can be used to study the Weil-Petersson geometry of the moduli space of Riemann surfaces. This leads to an efficient algorithm to compute the Weil-Petersson metric to arbitrary accuracy using Zamolodchikov’s recursion relation for conformal blocks. For example, we compute the metric on $\mathcal{M}_{0,4}$ numerically to high accuracy by considering Liouville theory on a sphere with four punctures. We numerically compute the eigenvalues of the Weil-Petersson Laplacian, and find evidence that they obey the statistics of a random matrix in the Gaussian Orthogonal Ensemble.

ARXIV EPRINT: [2210.08098](https://arxiv.org/abs/2210.08098)

Contents

1	Introduction and Discussion	1
2	Classical and quantum Liouville theory	3
2.1	The Liouville CFT	3
2.2	Semiclassical Liouville theory and hyperbolic geometry	5
3	The geometry of $\mathcal{M}_{0,4}$	7
3.1	Hyperbolic Geometry	8
3.2	Complex Geometry	9
4	The Weil–Petersson metric on $\mathcal{M}_{0,4}$	11
4.1	Metric near the boundary of moduli space	13
4.2	Perturbative expansion of the metric	14
4.3	Non-perturbative corrections to the metric	17
4.4	Comparison: the Weil–Petersson volume of $\mathcal{M}_{0,4}$	20
5	The spectrum on moduli space	22
5.1	The spectrum of eigenvalues	23
5.2	Asymptotic density of the spectrum: Weyl’s law	25
5.3	Level statistics: Nearest neighbor correlations	26
5.4	Level statistics: Spectral form factor	28
A	Numerical results for the eigenvalues	30
A.1	Numerical Data	30
A.2	On the accuracy of the eigenvalues	30

1 Introduction and Discussion

Two dimensional Conformal Field Theory (CFT) has proven to be a useful tool in both physics and mathematics, with applications ranging from the study of critical phenomena to string theory and topological quantum field theory. One of its most intriguing applications is to the geometry of surfaces. This is most clear in the Liouville conformal field theory introduced by Polyakov [1], which can be regarded as a quantum theory of geometry in two dimensions. The classical solutions of this theory are two dimensional surfaces of constant negative curvature, possibly with sources. This allows us to use Liouville theory to study the moduli space of Riemann surfaces, which can be regarded as the space of hyperbolic metrics (or alternately the space of conformal structures) on a surface of given topology. Our goal will be to use conformal field theory methods to study the Weil-Petersson (WP)

geometry of moduli space. Our main result is an efficient algorithm to approximate the Weil-Petersson metric to arbitrary accuracy.

Although we will restrict our attention to a relatively simple case – the moduli space $\mathcal{M}_{0,4}$ of the four-punctured sphere – this strategy works in general and can be used to study moduli spaces of surfaces both with and without boundary. A key role will be played by Zamolodchikov’s recursion relations for conformal blocks [2, 3], which leads to an approximation that converges extremely rapidly. For example, the first non-trivial order in this expansion gives a result for the volume of moduli space that is correct to one part in 10^{-7} . As an application of these results we will compute numerically the first 200 eigenvalues of the Weil-Petersson Laplacian on moduli space. We will verify that these obey the expected Weyl law governing the asymptotic behaviour of the spectrum of the Laplacian. We will also study the spacings of the eigenvalues, and show that these exhibit the expected behaviour for a chaotic system in the Gaussian Orthogonal Ensemble (GOE) universality class.

The relationship between Liouville theory and the classical and quantum geometry of surfaces has been discussed previously; early discussions include [4–6]. One major achievement in the study of Liouville theory was the remarkable solution – described in [7–12] – of the constraints of crossing symmetry to determine the three-point coefficients of the theory exactly. This opened the door to quantitative connections between Liouville theory and the geometry of surfaces. We particularly highlight the work of [13], which used the same technique that we will describe below, although to study a different quantity.

One of our central results is that these CFT techniques allow one to approximate the Weil-Petersson metric with sufficient accuracy that one can study the chaotic dynamics on moduli space explicitly. Although our focus is on the spectrum of the WP Laplacian, one could also study the classical dynamics of motion on moduli space. This subject has been of considerable interest in the mathematics literature, where various chaotic properties have been discussed previously (see e.g. [14, 15]). The study of quantum chaos also has a long history in the physics literature, where a generic Hamiltonian is expected to exhibit statistical properties which are governed by Random Matrix Theory (RMT) [16–18]. The most general ensemble of random matrices is the Gaussian Unitary Ensemble, which describes Hamiltonians without time-reversal symmetry. The GOE, which is the ensemble relevant for the WP Laplacian, describes Hamiltonians with time-reversal symmetry. RMT has also made an appearance in the study of gravitational systems, since black holes are expected to exhibit quantum chaos and therefore be described by RMT as well [19]. There is a substantial literature which studies the RMT behaviour of a variety of quantum mechanical systems, but examples where this can be studied in genuine field theories or gravitational systems are rare.¹

Our results have potential applications in quantum gravity. In particular, the Weil-Petersson Laplacian is a natural Hamiltonian acting on a phase space of metrics, so our computation can be regarded as a study of a simple model of quantum gravity based on the quantization of moduli space. This appears naturally in three dimensional theories of

¹See e.g. [20] for a recent example.

AdS gravity, where in a canonical formulation the phase space of a pure theory of gravity can be constructed from the moduli space of Riemann surfaces [21–25]. The computations in this paper are most simply related to so-called “chiral gravity” in AdS₃ [26], where the phase space is precisely the moduli space of Riemann surfaces endowed with the Weil-Petersson symplectic structure, as discussed recently in [24, 25].² It would be interesting to investigate whether, following [24], wave functions of the type we have constructed can be viewed as a class of black hole microstates. Our computations may also be applicable to two dimensional theories of gravity such as Jackiw-Teitelboim gravity in AdS₂, where the gravitational path integral can be written as an integral over the moduli space of Riemann surfaces with the Weil-Petersson volume form [27].

In §2 we briefly review a few important aspects of Liouville field theory and its relationship with the geometry of surfaces, before moving in §3 to a review of necessary features of the moduli space of curves. §4 contains the main computation, which uses the Zamolodchikov recursion relations to develop an accurate approximation to the Weil-Petersson metric, which is checked in a variety of ways. §5 applies this to a numerical computation of the eigenvalues of the Weil-Petersson Laplacian, along with a discussion of their properties. Appendix A lists the first 100 eigenvalues and includes a brief discussion of the numerical accuracy of these results.

2 Classical and quantum Liouville theory

In this section we review the basics of Liouville quantum field theory and its connection to the geometry of Riemann surfaces. We are brief, and only highlight a few aspects salient for our analysis in the coming sections. For more complete reviews of Liouville QFT, see e.g. [11, 28, 29].

2.1 The Liouville CFT

The action of Liouville theory on a Riemann surface Σ with complex coordinates (z, \bar{z}) (we use the conventions of [8]) is

$$S_L[\phi] := \int_{\Sigma} d^2z \sqrt{g} \left(\frac{1}{4\pi} g^{\alpha\beta} \partial_{\alpha} \phi \partial_{\beta} \phi + \mu e^{2b\phi} \right), \quad (2.1)$$

where μ is known as the Liouville cosmological constant. If the surface Σ has a boundary, this must be augmented by a certain choice of boundary conditions for ϕ at $\partial\Sigma$, but this will not be important for our discussion. The quantum theory described by this action is a conformal field theory with central charge $c = 1 + 6Q^2$, where $Q = b + 1/b$. The primary operators of this theory are the Liouville vertex operators $V_{\alpha}(z, \bar{z})$ with conformal dimension $\Delta_{\alpha} = \alpha(Q - \alpha)$ where

$$\alpha = \frac{Q}{2} + iP, \quad P \in \mathbb{R}^+.$$

²This is to be contrasted with general relativity in AdS₃, where the phase space is the cotangent bundle of moduli space.

We will refer to the parameter P as the Liouville momentum.

The quantum theory is characterized by the n -point correlation functions of primary operators:

$$\langle V_{\alpha_1}(z_1, \bar{z}_1) \dots V_{\alpha_n}(z_n, \bar{z}_n) \rangle. \quad (2.2)$$

Using operator product expansions these correlation functions can be reduced to expressions involving the three point function coefficients $C(\alpha_i, \alpha_j, \alpha_k)$ of primary operators and the Virasoro conformal blocks \mathcal{F}_P . For example, the four point function—which is the crucial ingredient we will use to study the geometry of $\mathcal{M}_{0,4}$ —can be represented as an integral over the Liouville momentum P of an internal operator exchanged in the s -channel as,

$$\langle V_{\alpha_4}(\infty, \infty) V_{\alpha_3}(1, 1) V_{\alpha_2}(x, \bar{x}) V_{\alpha_1}(0, 0) \rangle = \int dP C(\alpha_1, \alpha_2, \alpha) C(\alpha_3, \alpha_4, Q - \alpha) \left| \mathcal{F}_P \begin{bmatrix} \Delta_3 & \Delta_2 \\ \Delta_4 & \Delta_1 \end{bmatrix} (x) \right|^2, \quad (2.3)$$

where we have introduced the cross ratio

$$x = \frac{(z_1 - z_2)(z_3 - z_4)}{(z_1 - z_4)(z_3 - z_2)}.$$

The structure constants $C(\alpha_1, \alpha_2, \alpha_3)$ of Liouville have been determined explicitly by solving the constraints of conformal invariance and crossing symmetry, and are given by the so-called DOZZ formula [7, 8].

The 4-point Virasoro conformal block $\mathcal{F}_P \begin{bmatrix} \Delta_3 & \Delta_2 \\ \Delta_4 & \Delta_1 \end{bmatrix}$ captures the contributions to the four point function of an internal primary operator with Liouville momentum P along with all its Virasoro descendants. Closed form expressions for \mathcal{F}_P exist only in certain special cases, but we can efficiently compute its expansion around $x = 0$ to arbitrary order using the recursion relations of Zamolodchikov [3]. For example, the first two terms in the expansion are

$$\mathcal{F}_P \begin{bmatrix} \Delta_3 & \Delta_2 \\ \Delta_4 & \Delta_1 \end{bmatrix} = x^{\Delta - \Delta_2 - \Delta_1} \left(1 + \frac{(\Delta - \Delta_1 + \Delta_2)(\Delta + \Delta_3 - \Delta_4)}{2\Delta} x + \dots \right) \quad (2.4)$$

where $\Delta = \frac{Q^2}{4} + P^2$. These two terms represent the contributions to the correlation function from the exchange of the primary operator $V_{\alpha = \frac{Q}{2} + iP}$ and its L_{-1} descendant, respectively.

The decomposition (2.3) can be interpreted as a representation of a sphere with four holes by gluing together two pairs-of-pants along a common cuff. Each pair of pants is represented by a three point vertex $C(\alpha_1, \alpha_2, \alpha)$, and the integral over P is a sum over possible lengths of the cuff which are glued together. As we will review below, in the classical limit this is not just an analogy but an exact statement in hyperbolic geometry.

In addition to the correlation functions (2.2), it is possible to study correlation functions of Liouville theory on a general Riemann surface Σ . Even the vacuum amplitude—the partition function with no operator insertions—is non-trivial at higher genus, and has a conformal block decomposition related in a similar manner to the pair-of-pants decomposition of Σ .

2.2 Semiclassical Liouville theory and hyperbolic geometry

To make a connection to the classical geometry of constant negative curvature Riemann surfaces we will consider the semiclassical limit of the action (2.1). This is the $c \rightarrow \infty$ (or $Q \rightarrow \infty$) limit. In this limit it is convenient to introduce a new field, $\tilde{\phi} := 2b\phi$ and the parameter $\tilde{\mu} := \mu b^2$, so that the action of equation (2.1) takes the form

$$S_L[\tilde{\phi}] := \frac{1}{b^2} \int_{\Sigma} d^2z \sqrt{g} \left(\frac{1}{16\pi} g^{\alpha\beta} \partial_{\alpha} \tilde{\phi} \partial_{\beta} \tilde{\phi} + \tilde{\mu} e^{\tilde{\phi}} \right). \quad (2.5)$$

We will then take the semiclassical limit $b \rightarrow 0$ with $\tilde{\mu}$ is fixed. We see from (2.5) that the parameter b plays the role of $\sqrt{\hbar}$. With a flat reference metric g (which we can enforce with an appropriate choice of boundary condition) the classical equation of motion for $\tilde{\phi}$ is Liouville's equation

$$\partial \bar{\partial} \tilde{\phi} = 2\pi \tilde{\mu} e^{\tilde{\phi}}. \quad (2.6)$$

When we take this semiclassical limit we will also scale the dimensions of the Liouville vertex operators by taking $p = \frac{P}{Q}$ fixed as $b \rightarrow 0$. So the dimension will scale as

$$\Delta_{\alpha} = \alpha(Q - \alpha) = \frac{Q^2}{4}(1 - \xi^2) \approx \frac{1}{4b^2}(1 - \xi^2), \quad (2.7)$$

in the semiclassical limit, where we have defined $\xi := i\frac{Q}{2}P$. In particular, we define the Liouville momentum p in the semiclassical limit via the relation $\alpha = \frac{Q}{2} + iP := \frac{Q}{2}(1 + 2ip)$. We also will sometimes refer to the conformal weight of a primary operator in the semiclassical limit by the rescaled dimension $\delta := \frac{\Delta}{Q^2} = \frac{1 - \xi^2}{4}$, which is also used in [13]. Note that in the semiclassical limit, these correspond to heavy operators, as for fixed ξ, δ , the original dimensions Δ scale like Q^2 .

When we take the semiclassical limit in this way, the n -point correlation function is given by a classical action,

$$\langle V_{\alpha_1}(z_1, \bar{z}_1) \dots V_{\alpha_n}(z_n, \bar{z}_n) \rangle_{b \rightarrow 0} \rightarrow \exp \left(-\frac{1}{b^2} S_L^{cl}[\tilde{\phi}_*] \right), \quad (2.8)$$

where $S_L^{cl}[\tilde{\phi}_*]$ is the action (4.2) evaluated at $\tilde{\phi}_*$, the unique solution of (2.6) with certain prescribed boundary conditions on $\tilde{\phi}(z, \bar{z})$ at the locations of the vertex operators z_1, \dots, z_n on Σ . (See, e.g., [12, 13] for the precise form of the boundary conditions.)

The connection to hyperbolic geometry then arises from the fact that the classical solution to (2.6), $\tilde{\phi}_*(z, \bar{z})$, furnishes a unique metric of constant negative curvature on the Riemann surface Σ with n elliptic or parabolic singularities (cone points or punctures, resp.) at the set of points $\{z_1, \dots, z_n\}$. In particular, the metric,

$$ds^2 = e^{\tilde{\phi}_*(z, \bar{z})} |dz|^2, \quad (2.9)$$

has constant negative curvature, because the Ricci scalar

$$R = -4e^{-\tilde{\phi}_*} \partial \bar{\partial} \tilde{\phi}_*, \quad (2.10)$$

becomes constant $R = -8\pi\tilde{\mu}$ when the Liouville equation of motion is satisfied.

Note that the type of singularity which appears at the point z_i depends on the semiclassical conformal weight δ_i of $V_{\alpha_i}(z_i)$ in the following way: for $0 < \xi_i < 1$ ($0 < \delta_i < 1/4$), there is a conical singularity of opening angle $2\pi\xi_i$ at the point z_i . Vertex operators where ξ takes imaginary values correspond to holes. In terms of the hyperbolic metric, when $\xi_i = \frac{i\ell_i}{2\pi}$, corresponding to

$$\delta_i = \frac{1}{4} + \frac{1}{4} \left(\frac{\ell_i}{2\pi} \right)^2, \quad (2.11)$$

there is a hole with a geodesic boundary of length ℓ_i . The special case when $\xi_i \rightarrow 0$ ($\delta_i \rightarrow 1/4$) will be of particular interest for us, as in this case there is a puncture at the point z_i .

We will be interested in understanding the geometry of $\mathcal{M}_{0,4}$, the moduli space of four-punctured spheres, so we begin by considering the semiclassical limit of the four point function (2.3). In order to compute the semiclassical limit of the four point function, we need to know both the semiclassical behavior of the three point function $C(\alpha_1, \alpha_2, \alpha_3)$, as well as the conformal block \mathcal{F}_P .

In the semi-classical limit the DOZZ formula for the structure constants reduces to an exponential of the classical Liouville action of the form (see e.g. [8, 30])

$$C(\alpha_1, \alpha_2, \alpha_3) \approx e^{-\frac{1}{b^2} S_3^{cl}(\delta_1, \delta_2, \delta_3)}, \quad (2.12)$$

where $S_3^{cl}(\delta_1, \delta_2, \delta_3)$ is the classical 3-point action of vertex operators with dimensions $\delta_1, \delta_2, \delta_3$ on the sphere. Furthermore, the conformal block was conjectured to take a similar exponential form in the semiclassical limit by Zamolodchikov [31], which has since been proven [32],

$$\mathcal{F}_P \begin{bmatrix} \Delta_3 & \Delta_2 \\ \Delta_4 & \Delta_1 \end{bmatrix} (x) \approx \exp \left[\frac{1}{b^2} f_p \begin{bmatrix} \delta_3 & \delta_2 \\ \delta_4 & \delta_1 \end{bmatrix} (x) \right], \quad (2.13)$$

where f_p is called the ‘‘classical conformal block.’’ Although closed form expressions for f_p are not known, it can be evaluated in an expansion at small x simply by taking the large c limit of the expansion in equation (2.4).

Since both the structure constants and the conformal block take an exponential form, the semiclassical limit of the four point function can be written as,

$$\begin{aligned} & \langle V_{\alpha_4}(\infty, \infty) V_{\alpha_3}(1, 1) V_{\alpha_2}(x, \bar{x}) V_{\alpha_1}(0, 0) \rangle \\ & \approx \int dp \exp \left[-\frac{1}{b^2} \left(S_3^{cl}(\delta_1, \delta_2, 1/4 + p^2) + S_3^{cl}(1/4 + p^2, \delta_3, \delta_4) - 2\text{Re} f_p \begin{bmatrix} \delta_3 & \delta_2 \\ \delta_4 & \delta_1 \end{bmatrix} (x) \right) \right], \end{aligned} \quad (2.14)$$

where p is the Liouville momentum of the internal vertex operator. In the semiclassical limit we may approximate this integral using the method of saddle points, with saddle point determined by the equation

$$\frac{d}{dp} \left(S_3^{cl}(\delta_1, \delta_2, 1/4 + p^2) + S_3^{cl}(1/4 + p^2, \delta_3, \delta_4) - 2\text{Re} f_p \begin{bmatrix} \delta_3 & \delta_2 \\ \delta_4 & \delta_1 \end{bmatrix} (x) \right) \Big|_{p=p_s} = 0. \quad (2.15)$$

The solution $p = p_s(x, \bar{x})$ to this equation determines the saddle point value of the internal Liouville momentum in terms of the cross ratio. Finally, inserting this saddle point value into the action, we arrive at the semiclassical limit of the Liouville four point function,

$$\langle V_{\alpha_4}(\infty, \infty) V_{\alpha_3}(1, 1) V_{\alpha_2}(x, \bar{x}) V_{\alpha_1}(0, 0) \rangle \approx e^{-\frac{1}{i^2} S_L^{cl}(x, \bar{x})}, \quad (2.16)$$

$$S_L^{cl}(x, \bar{x}) := (S_3^{cl}(\delta_1, \delta_2, 1/4 + p_s^2) + S_3^{cl}(1/4 + p_s^2, \delta_3, \delta_4) - 2\text{Re} f_{p_s} \begin{bmatrix} \delta_3 & \delta_2 \\ \delta_4 & \delta_1 \end{bmatrix})(x),$$

which is a function of the cross ratio x . In the context of the moduli space $\mathcal{M}_{0,4}$ this classical action has an important interpretation: it is the Kähler potential for the Weil-Petersson metric (see e.g. [33]). We will discuss this in more detail below.

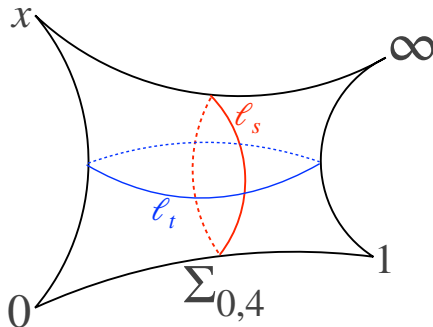


Figure 1: Illustration of a four-punctured Riemann sphere $\Sigma_{0,4}$. In blue and red are the minimal s - and t -channel geodesics, of lengths ℓ_s and ℓ_t , respectively.

We note that the saddle point momentum p_s has the following physical interpretation—the action of equation (2.16) in the semiclassical limit describes a process where an operator of dimension $\delta_s = \frac{1}{4} + p_s^2$ is exchanged in the s -channel. From equation (2.11), we see that this corresponds to the length $\ell_s = 4\pi p_s$ of the minimal s -channel geodesic on the four-punctured sphere, separating the two punctures (or conical singularities) at 0 and x from the two punctures located at 1 and ∞ . Similarly, a solution for the saddle point momentum in the t -channel or u -channel corresponds to lengths ℓ_t and ℓ_u of minimal geodesics around the punctures at 1 and x or ∞ and x , respectively. See Figure 1 for an illustration of the minimal s -channel and t -channel geodesics on the four-punctured sphere.

In §4 we will specialize to the case of a sphere with four punctures by taking $\delta_i = \frac{1}{4}$, $i = 1, \dots, 4$, and study the saddle point equation (2.15). Using Zamolodchikov’s recursion relations for the conformal blocks f_p , we will numerically approximate the saddle point action, which will allow us to numerically compute the Weil-Petersson metric on $\mathcal{M}_{0,4}$ to very high accuracy.

3 The geometry of $\mathcal{M}_{0,4}$

Before proceeding, we will briefly summarize some aspects of the geometry of the moduli space $\mathcal{M}_{0,4}$ of the four-punctured sphere.

3.1 Hyperbolic Geometry

We begin by recalling the construction of a Riemann surface with n punctures $\Sigma_{0,n}$ as a quotient of the upper half plane. Let \mathbb{H} be the upper half-plane with coordinates $\{(x, y) | x \in \mathbb{R}, y > 0\}$ and hyperbolic metric,

$$ds^2 = \frac{dx^2 + dy^2}{y^2}. \quad (3.1)$$

The isometry group $PSL(2, \mathbb{R})$ has a natural action on \mathbb{H} given by,

$$z \mapsto \frac{az + b}{cz + d}, \quad \begin{pmatrix} a & b \\ c & d \end{pmatrix} \in PSL(2, \mathbb{R}),$$

where $z = x + iy$. Geodesics are circular arcs which intersect the real axis perpendicularly. The geodesic distance $d(z, w)$ between two points $z, w \in \mathbb{H}$ is fully determined by the trace of the matrix $g = \begin{pmatrix} a & b \\ c & d \end{pmatrix} \in PSL(2, \mathbb{R})$ which maps $z \mapsto w = \frac{az+b}{cz+d}$ as,

$$\cosh \frac{d(z, w)}{2} = \frac{1}{2} \text{Tr} g. \quad (3.2)$$

The uniformization theorem implies that a Riemann sphere with n punctures $\Sigma_{0,n}$ is biholomorphic to the quotient \mathbb{H}/G where \mathbb{H} is endowed with the metric (3.1) and $G < PSL(2, \mathbb{R})$ is a Fuchsian (discrete) subgroup. The group G is isomorphic to the fundamental group of $\Sigma_{0,n}$. Furthermore, it has n generators γ_i , $i = 1, \dots, n$, which satisfy $|\text{Tr} \gamma_i| = 2$, coming from the fact that each puncture corresponds to a length zero geodesic boundary of $\Sigma_{0,n}$. Moreover, the generators satisfy the relation

$$\gamma_1 \gamma_2 \dots \gamma_n = \mathbf{1}_{2 \times 2}, \quad (3.3)$$

due to the fact that any circle which encloses all n punctures is contractible.

For any pair of punctures z_i and z_j , there is a unique closed geodesic of the hyperbolic metric on $\Sigma_{0,n}$ which encloses precisely z_i and z_j but none of the other $n - 2$ punctures. This geodesic has length $d_{ij} := d(z_i, z_j)$ where

$$\cosh \frac{d_{ij}}{2} = \frac{1}{2} |\text{Tr} \gamma_i \gamma_j|.$$

Specializing to the case of four punctures, it is clear that a choice of $\Sigma_{0,4}$ depends on two real parameters³, so the moduli space $\mathcal{M}_{0,4}$ is one-complex dimensional.

This moduli space enjoys several remarkable properties. In particular, it is a complex manifold with a natural symplectic structure – the Weil-Petersson symplectic structure – with respect to which $\mathcal{M}_{0,4}$ is a Kähler manifold, with Kähler potential equal to the Liouville action $S_L^{cl}(x, \bar{x})$.

³Each generator $a_i \in PSL(2, \mathbb{R})$ contains two real degrees of freedom due to the constraint $|\text{Tr} a_i| = 2$. The additional constraint (3.3) removes an additional 3 parameters. Finally, an overall conjugation symmetry by an element of $PSL(2, \mathbb{R})$ removes an additional three degrees of freedom, such that we are left with $4 \times 2 - 3 - 3 = 2$ real parameters.

There are several natural choices of coordinates for the moduli space $\mathcal{M}_{0,4}$, each of which are useful for illustrating different properties of the moduli space. For example, a simple set of coordinates are the lengths ℓ_s and ℓ_t of the minimal length geodesics in the s - and t -channel, as in Figure 1. If we think of the surface as the quotient \mathbb{H}/G , then these lengths are just given by formula (3.2) for the corresponding elements of G . One advantage of these coordinates is that the Weil-Petersson symplectic structure can be explicitly computed, and takes the form

$$\omega^{WP} = \frac{1}{\cos \theta} d\ell_s \wedge d\ell_t, \quad (3.4)$$

where θ is the angle of intersection between the two geodesics.

Another related set of coordinates are the Fenchel-Nielsen coordinates, which are defined as follows. We start by noticing that there is a one-real parameter family of metrics on the disk with two punctures and a boundary that is a hyperbolic geodesic; this family of metrics is labelled by the hyperbolic length ℓ of the boundary circle. We can then construct a four-punctured sphere by gluing two of these disks together along their hyperbolic boundaries. For example, we can think of the two disks as the left- and right-hand sides of Figure 1, and identify ℓ as the s -channel length ℓ_s . We are also free to glue together these disks with any relative angle, meaning that there is an additional twist parameter θ_s . The pair (ℓ_s, θ_s) are the Fenchel-Nielsen coordinates. In these coordinates the Weil-Petersson symplectic structure takes the very simple form,

$$\omega^{WP} = d\ell_s \wedge d\theta_s. \quad (3.5)$$

One important point is that the coordinates described above are not unique. For example, by construction the twist coordinate is periodic: $\theta_s \sim \theta_s + \ell_s$. A rotation of the angle θ_s by this amount is known as a Dehn twist. Indeed, one could choose *any* closed geodesic on $\Sigma_{0,4}$ and consider the corresponding Dehn twist. The coordinates (ℓ_s, θ_s) (or (ℓ_s, ℓ_t)) would transform in a complicated way under this Dehn twist, but these two different values of the coordinates would in fact describe the same surface $\Sigma_{0,4}$. This gives the moduli space the structure of a quotient. In particular, the group generated by the Dehn twists is the mapping class group, the group of diffeomorphisms modulo those which are continuously connected to the trivial diffeomorphism. The moduli space $\mathcal{M}_{0,4}$ can be viewed as a quotient of Teichmüller space (the simply connected space parameterized by all real values of the Fenchel-Nielsen coordinates) by the mapping class group. Much of the difficulty in the study of moduli space comes from the complicated behaviour of this group action.

3.2 Complex Geometry

One advantage of working with the geodesic length coordinates is that the Weil-Petersson symplectic structure can be explicitly computed. However, these coordinates obscure the fact that $\mathcal{M}_{0,4}$ is a complex manifold. To see this, another natural choice of coordinate on moduli space is the complex cross-ratio x . If $\{z_1, z_2, z_3, z_4\} \subset \mathbb{C}^*$ are the locations of

four marked points on the Riemann sphere, there exists a unique $SL(2, \mathbb{C})$ transformation which maps this set of points to $\{x, 0, 1, \infty\} \subset \mathbb{C}^*$, where

$$x = \frac{(z_1 - z_2)(z_3 - z_4)}{(z_1 - z_4)(z_3 - z_2)}.$$

This x is a complex coordinate on the moduli space $\mathcal{M}_{0,4}$. The moduli space then inherits the usual complex structure from \mathbb{C} .

The Weil-Petersson metric is the Kähler metric associated with the symplectic form ω^{WP} . Since this symplectic form is easily computed in the length-twist coordinates, in principle one could compute the metric exactly provided one knew how to compute the length $\ell_s(x, \bar{x})$ as a function of the cross-ratio. Unfortunately $\ell_s(x, \bar{x})$ does not have a simple closed form, although one can study the problem perturbatively in an expansion near $x = 0$. We will use essentially this method in the next section, although we will find it more convenient to work directly with the Liouville action rather than the length coordinates.

Note that our original moduli space is the space of labelled points, so naturally admits the action of the group S_4 which permutes the four points. All of the structures which we are considering are invariant under this action. The cross ratio x is invariant under the subgroup $\mathbb{Z}_2 \times \mathbb{Z}_2 \in S_4$ which contains the products of two elements of order two in S_4 . The remaining permutations, which can be taken to live in the quotient $S_3 = S_4 / (\mathbb{Z}_2 \times \mathbb{Z}_2)$, act on x as the anharmonic transformations,

$$S_3 : x \rightarrow \left\{ x, 1 - x, \frac{1}{x}, \frac{1}{1 - x}, \frac{x}{x - 1}, \frac{x - 1}{x} \right\}. \quad (3.6)$$

These are generated by $x \rightarrow 1 - x$ and $x \rightarrow 1/x$, which are the usual crossing transformations that interchange the s -channel with the t - and u -channels, respectively.

The anharmonic group S_3 is order 6, so this action divides the complex plane into six fundamental domains. Thus, rather than taking $\mathcal{M}_{0,4}$ to be the full complex x plane, we may take our moduli space to be a 6-fold cover of a fundamental domain for this S_3 action. We will take as our fundamental domain,

$$\Delta = \{\text{Re}(x) < 1/2, |x - 1| < 1\} \subset \mathbb{C}. \quad (3.7)$$

This is a convenient choice for any computation which involves an approximation scheme which is valid near $x = 0$ but is expected to break down near the other singular points at $x = 1$ and $x = \infty$, such as an s -channel expansion.

Zamolodchikov's q coordinate

As we will see when we return to the connection to Liouville theory, following [3], it will be useful to define a new coordinate on moduli space, q , as

$$q := \exp \left(-\pi \frac{K(1 - x)}{K(x)} \right), \quad (3.8)$$

where x is the cross-ratio coordinate discussed above, and

$$K(x) := \int_0^1 \frac{dt}{\sqrt{(1-t^2)(1-xt^2)}}$$

is the complete elliptic integral of the first kind. For $x \in \mathbb{C}^* \setminus \{0, 1, \infty\}$, it follows that $|q(x)| < 1$. Furthermore, the map $x \mapsto q(x)$ furnishes a uniformization of the 3-punctured sphere by the unit disk \mathbb{D} with a hyperbolic metric. Near the boundary of moduli space $x \rightarrow 0$, we have $q \sim x/16$.

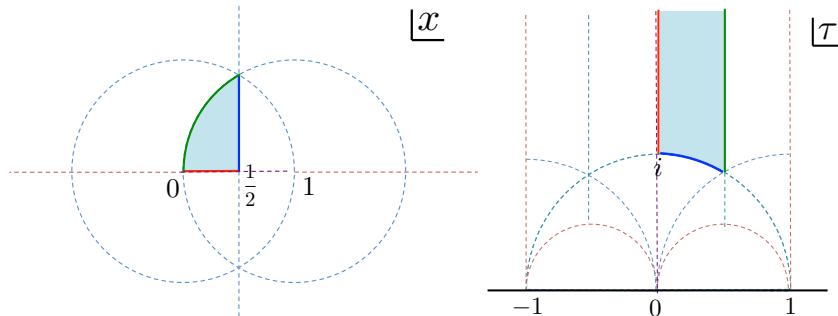


Figure 2: The moduli space $\mathcal{M}_{0,4}$ in the cross-ratio coordinate x (left) and the τ coordinate (right). The shaded region corresponds to half of the fundamental domain, and will later become the region on which we solve Laplace’s equation. The full fundamental domain is found by considering the union of the red boundary line, the shaded region, and the reflection of the shaded region over the red line.

Finally, it will also be convenient to express q as a function of a variable $\tau \in \mathbb{H}$, where $q = \exp(\pi i \tau)$, and consider τ as a complex coordinate on $\mathcal{M}_{0,4}$. It follows that in terms of the cross-ratio coordinate, $\tau = i \frac{K(1-x)}{K(x)}$. (Half-)fundamental domains for the x and τ coordinates are pictured in Figure 2.

4 The Weil–Petersson metric on $\mathcal{M}_{0,4}$

In this section, we will study the classical Liouville action $S_L^{cl}(x, \bar{x})$ for a sphere with four punctures using the saddle point equation (2.15). Since $S_L^{cl}(x, \bar{x})$ is a Kähler potential⁴ for $\mathcal{M}_{0,4}$ this will allow us to study the the Weil–Petersson metric on the moduli space $\mathcal{M}_{0,4}$. Our goal is to achieve an accurate numerical approximation for the metric.

Specifically, the Weil-Petersson metric on $\mathcal{M}_{0,4}$ is given by

$$g_{x\bar{x}} = -4\pi \partial_x \partial_{\bar{x}} S_L^{cl}(x, \bar{x}), \tag{4.1}$$

where $S_L^{cl}(x, \bar{x})$ is the classical Liouville action evaluated at the saddle point momentum $p_s(x)$. Once we have specialized to the case of four punctures, corresponding to $\delta_i = \frac{1}{4}$, $i =$

⁴This was proven in [33], and also holds when the four singularities are elliptic (cone points) rather than parabolic (punctures).

1, . . . 4, we can write the classical action as

$$S_L^{cl}(x, \bar{x}) = 2S_3^{cl}(\frac{1}{4}, \frac{1}{4}, \frac{1}{4} + p^2) - 2\text{Re} f_p \left[\begin{matrix} \frac{1}{4} & \frac{1}{4} \\ \frac{1}{4} & \frac{1}{4} \end{matrix} \right] (x), \quad (4.2)$$

where S_3^{cl} is the 3-point classical action and f_p is the classical conformal block.

Furthermore, the 3-point classical action is explicitly given by [8]

$$S_3^{cl}(\frac{1}{4}, \frac{1}{4}, \frac{1}{4} + p^2) = \frac{1}{2} \log 2 + 2F(\frac{1}{2} + ip) + 2F(\frac{1}{2} - ip) - 2F(0) + H(2ip) + \pi p, \quad (4.3)$$

where we define

$$\begin{aligned} F(x) &:= \int_{\frac{1}{2}}^x dy \log \frac{\Gamma(y)}{\Gamma(1-y)} = \psi^{(-2)}(x) + \psi^{(-2)}(1-x) - 2\psi^{(-2)}(\frac{1}{2}), \\ H(x) &:= \int_0^x dy \log \frac{\Gamma(-y)}{\Gamma(y)} = -\psi^{(-2)}(x) - \psi^{(-2)}(-x), \end{aligned} \quad (4.4)$$

and $\psi^{(n)}(x)$ is the n -th polygamma function. Plugging this in to (2.15), we see that the saddle point momentum $p_s(x)$ must satisfy the differential equation,

$$\begin{aligned} \frac{d}{dp} S_L^{cl}(x, \bar{x}; p) \Big|_{p=p_s} &= \frac{d}{dp} \left[2S_3^{cl}(\frac{1}{4}, \frac{1}{4}, \frac{1}{4} + p^2) - 2\text{Re} f_p \left[\begin{matrix} \frac{1}{4} & \frac{1}{4} \\ \frac{1}{4} & \frac{1}{4} \end{matrix} \right] (x) \right] \Big|_{p=p_s} \\ &= -\pi + 2i \log \frac{\Gamma(1-2ip_s)\Gamma^2(\frac{1}{2}+ip_s)}{\Gamma(1+2ip_s)\Gamma^2(\frac{1}{2}-ip_s)} - \text{Re} \frac{\partial}{\partial p} f(p, x) \Big|_{p=p_s} = 0, \end{aligned} \quad (4.5)$$

where we have defined the notation $f(p, x)$ by

$$\begin{aligned} f(p, x) &:= f_p \left[\begin{matrix} \frac{1}{4} & \frac{1}{4} \\ \frac{1}{4} & \frac{1}{4} \end{matrix} \right] (x) \\ &= \left(p^2 - \frac{1}{4} \right) \log x + \left(\frac{1}{8} + \frac{p^2}{2} \right) x + \left(\frac{9}{128} + \frac{13}{64} p^2 + \frac{1}{1024(1+p^2)} \right) x^2 + O(x^3) \end{aligned} \quad (4.6)$$

Here we have included the first few terms in the expansion of the classical conformal block.

In the rest of this section, we explicitly solve (4.5) for the saddle point momentum p_s to increasing degrees of accuracy using Zamolodchikov’s recursion for f_p , and use this to compute a numerical approximation to the Weil–Petersson metric $g_{x\bar{x}}$. In §4.1, we compute the metric near the boundary of moduli space, where the cross-ratio coordinate $x \rightarrow 0$. In §4.2, we derive what we term a “perturbative” expansion of the saddle point momentum in terms of a variable $\varepsilon(q, \bar{q}) \sim -1/\log(q\bar{q})$, where q is the coordinate defined in §3, which in principle allows us to compute the metric to arbitrarily high accuracy in the 3-point action, at leading order in the expansion of f_p . We improve upon this in §4.3, where we outline a method to compute the saddle point momentum, and thus the metric, up to any desired order in the expansion of f_p . As the expansion of f_p amounts to an expansion of $\exp(-1/\varepsilon(q, \bar{q}))$, we dub these “non-perturbative” corrections. Finally, we also verify that our numerical approximation to the metric reproduces known quantities, such as the volume of $\mathcal{M}_{0,4}$ and geodesic lengths, to a very high degree of accuracy in §4.4.

4.1 Metric near the boundary of moduli space

We first analyze the behavior of the Weil-Petersson metric $g_{x\bar{x}}$ in the limit of small cross-ratio coordinate, $x \rightarrow 0$, which corresponds to a boundary of $\mathcal{M}_{0,4}$. This also corresponds to the limit where the geodesic length $\ell_s = 4\pi p_s \rightarrow 0$. In this limit the three-point function has the expansion,

$$S_3^{cl} \left(\frac{1}{4}, \frac{1}{4}, \frac{1}{4} + p^2 \right) \sim \log 2 + 4\psi^{(-2)}(1/2) - 2\psi^{(-2)}(1) - \pi p + 8p^2 \log 2 + \mathcal{O}(p^3). \quad (4.7)$$

This follows from the expansion of the functions,

$$\begin{aligned} F(1/2 + ip) &\sim -\psi(1/2)p^2 + \mathcal{O}(p^3), \\ H(2ip) &\sim -2\pi p - 4\gamma p^2 + \mathcal{O}(p^3), \end{aligned}$$

near $p = 0$, where $\psi(y)$ is the digamma function, which satisfies $\psi(1/2) + \gamma = -2 \log 2$, as well as the expansion of the conformal block near $p = 0$,

$$f(p, x) \sim 1 - \frac{1}{4} \log x + p^2 \log x + \mathcal{O}(p^3). \quad (4.8)$$

Therefore, at leading order in p , we can write the saddle point equation as,

$$\left. \frac{\partial}{\partial p} (2S_3^{cl}(\frac{1}{4}, \frac{1}{4}, \frac{1}{4} + p^2) - f(p, x) - \bar{f}(p, \bar{x})) \right|_{p=p_s} = -2\pi + 32p_s \log 2 - 2p_s \log x - 2p_s \log \bar{x} + \mathcal{O}(p_s^2) = 0. \quad (4.9)$$

The solution to this equation at leading order

$$p_s(x, \bar{x}) = \frac{\pi}{-\log(\bar{x}x) + 16 \log 2}, \quad (4.10)$$

gives the value of the s -channel saddle point momentum at leading order near the boundary of moduli space, $x \rightarrow 0$. Note that when $|x| \ll 2^{-r}$, we can ignore the factor of $16 \log 2$, and the length of the s -channel geodesic is approximately

$$\ell_s = 4\pi p_s \approx \frac{4\pi^2}{\log \frac{2^{16}}{x\bar{x}}} \approx \frac{2\pi^2}{\log \frac{1}{|x|}}. \quad (4.11)$$

Plugging the saddle point momentum p_s back into the expression (4.2) for the Liouville action, we find

$$S_L^{cl}(x, \bar{x}) = -2 + 2 \log 2 - 4F(0) + \frac{1}{4} \log x + \frac{1}{4} \log \bar{x} + \frac{\pi^2}{-\log(2^{-16}x\bar{x})}, \quad (4.12)$$

in the limit $x \rightarrow 0$. This leads to the following leading order behavior of the Weil-Petersson metric,

$$\boxed{g_{x\bar{x}} = -4\pi \partial_x \partial_{\bar{x}} S_L^{cl}(x, \bar{x}) = \frac{8\pi^3}{x\bar{x} \log^3(\frac{2^{16}}{x\bar{x}})}} \quad (4.13)$$

near the boundary of moduli space, $x \rightarrow 0$. This formula matches the expression for the Weil-Petersson metric near the boundary of moduli space derived by Wolpert [34] (section

2.3). Indeed, it is straightforward to check that this matches Wolpert's formula for the symplectic structure $\omega^{WP} = d\theta \wedge d\ell$ if one uses the fact (proven in [34]) that near the boundary of moduli space

$$\ell \sim \frac{2\pi^2}{\log(1/|q|)}, \quad \frac{2\pi\theta}{\ell} \sim \arg(q).$$

4.2 Perturbative expansion of the metric

Our method will be to compute the metric in a perturbative expansion in the s -channel Liouville momentum around $p_s = 0$. As we saw previously, the limit $p_s \rightarrow 0$ corresponds to the boundary of $\mathcal{M}_{0,4}$ in the cross-ratio coordinate, $x \rightarrow 0$. This is a good approximation only for a small range of x , since the Taylor expansion for $f(p, x)$ converges only when $x < 1$. So instead of using the cross-ratio coordinate we will study the saddle-point equation as a function of the variable $q(x)$, defined in (3.8). The advantage is that $f(p, x)$ will then rapidly converge at all points $x \in \mathbb{C}$, except for small neighborhoods around $x = 1, \infty$.

The leading order metric

We begin by writing the leading order expansion of the conformal block as,

$$f(p, x) \sim -\frac{1}{4} \log x - \frac{1}{4} \log(1-x) - \frac{7}{4} \log \frac{2}{\pi} K(x) + p^2 \log 16 + p^2 \log q(x) + \mathcal{O}(p^3), \quad (4.14)$$

so that we can write the Liouville action up to $\mathcal{O}(p^2)$ as

$$\begin{aligned} S_L^{cl}(x, \bar{x}) &= G(x) + \bar{G}(\bar{x}) + p^2 \log \frac{2^8}{q(x)\bar{q}(\bar{x})} - 2\pi p \\ &= G(x) + \bar{G}(\bar{x}) + \log \frac{2^8}{q(x)\bar{q}(\bar{x})} \left(p - \frac{\pi}{\log \frac{2^8}{q(x)\bar{q}(\bar{x})}} \right)^2 - \frac{\pi^2}{\log \frac{2^8}{q(x)\bar{q}(\bar{x})}}, \end{aligned} \quad (4.15)$$

where we have defined

$$G(x) := \log 2 + 4\psi^{(-2)}(1/2) - 2\psi^{(-2)}(1) + \frac{1}{4} \log x + \frac{1}{4} \log(1-x), \quad (4.16)$$

which is a holomorphic function of x , and thus will not contribute in the computation of the metric. It is clear from the expression (4.15) that at leading order the saddle-point value of the momentum is,

$$p_s(x) = \frac{\pi}{\log \frac{2^8}{q(x)\bar{q}(\bar{x})}}, \quad (4.17)$$

which corresponds to the following length of the s -channel geodesic,

$$l_s = 4\pi p_s \approx \frac{4\pi^2}{\log \frac{2^8}{q\bar{q}}} \underset{q \rightarrow 0}{\approx} \frac{2\pi^2}{\log \frac{1}{|q|}}. \quad (4.18)$$

Let $g_{q\bar{q}}$ be the Weil–Peterson metric in the q -coordinate, so that $ds^2 = 2g_{q\bar{q}}dq d\bar{q}$. After evaluating the classical action at the value of p_s at leading order in q (4.17), and taking two derivatives, we arrive at the following expression for the metric,

$$\boxed{g_{q\bar{q}} = \frac{8\pi^3}{q\bar{q}(\log \frac{2^8}{q\bar{q}})^3}}. \quad (4.19)$$

This is the result for $g_{q\bar{q}}$ at leading order in the q -expansion of $f(p, x)$. Note that (4.19) can be expanded in terms of $-\log(q\bar{q})$ as,

$$g_{q\bar{q}} = \frac{8\pi^3}{[-\log(q\bar{q})]^3} \left[1 + \frac{3\log 2^8}{\log(q\bar{q})} + \dots \right]. \quad (4.20)$$

This will contain infinitely many corrections in the $\frac{1}{\log(q\bar{q})}$ expansion.

The metric at next-to-leading order

To find the metric at next-to-leading order, we begin by expanding $S_3^{cl}(\frac{1}{4}, \frac{1}{4}, \frac{1}{4} + p^2)$ to $\mathcal{O}(p^4)$, so that the full action takes the form

$$S_L^{cl}(q, \bar{q}; p) \sim -2\pi p + 8p^2 \log 2 - 4\zeta(3)p^4 - p^2 \log(q\bar{q}) + G(q) + \bar{G}(\bar{q}) + \mathcal{O}(p^5), \quad (4.21)$$

where we have suppressed the dependence of q on x , and, as previously, $G(q)$ is a holomorphic function of q and independent of p . At this order in p , the saddle point equation becomes,

$$\left. \frac{\partial S_L^{cl}(q, \bar{q}; p)}{\partial p} \right|_{p=p_s} \sim -2\pi + 32p_s \log 2 - 16\zeta(3)p_s^3 - 4p_s \log 16 - 2p_s \log q\bar{q} = 0, \quad (4.22)$$

which has the solution,

$$p_s \sim \frac{\pi}{\log \frac{2^8}{q\bar{q}}} + \frac{8\zeta(3)\pi^3}{(\log \frac{2^8}{q\bar{q}})^4}. \quad (4.23)$$

At this point, it will be convenient to define an expansion parameter $\varepsilon(q, \bar{q}) := \frac{\pi}{\log \frac{2^8}{q\bar{q}}}$, which captures the leading order value of the saddle-point momentum, and such that p_s is given by a power series in $\varepsilon(q, \bar{q})$ of the form,

$$p_s \sim \varepsilon(q, \bar{q}) + \frac{8\zeta(3)}{\pi} \varepsilon(q, \bar{q})^4 + \dots. \quad (4.24)$$

Plugging this value of p_s back into the Liouville action, we find the on-shell value takes the form,

$$S_L^{cl}(q, \bar{q}; p_s(q)) = -\pi \varepsilon(q, \bar{q}) - 4\zeta(3) \varepsilon(q, \bar{q})^4 + \dots = -\frac{\pi^2}{\log \frac{2^8}{q\bar{q}}} - 4\zeta(3) \frac{\pi^4}{(\log \frac{2^8}{q\bar{q}})^4} + \dots. \quad (4.25)$$

Taking two derivatives allows us to compute the Weil–Petersson metric at next-to-leading order in $\varepsilon(q, \bar{q})$, and we find,

$$\boxed{g_{q\bar{q}} = -4\pi \partial_q \partial_{\bar{q}} S_L^{cl}(q, \bar{q}) = \frac{8\pi^3}{q\bar{q} (\log \frac{2^8}{q\bar{q}})^3} \left[1 + \frac{40\pi^2 \zeta(3)}{(\log \frac{2^8}{q\bar{q}})^3} + \dots \right]}, \quad (4.26)$$

which includes the first correction to the leading order result found in (4.19).

A perturbative expansion for $g_{q\bar{q}}$

Now we outline a general method for computing the metric $g_{q\bar{q}}$ to arbitrary order in $\varepsilon(q, \bar{q})$, at leading order in the expansion of $f(p, x)$. We begin by expanding the Liouville action as,

$$S_L^{cl}(q, \bar{q}; p) = -2\pi p + 8p^2 \log 2 - p^2 \log(q\bar{q}) + 16p^4 \sum_{k=1}^{\infty} \frac{(-1)^{k-1} (1-4^k) \zeta(2k+1)}{(2k+1)(2k+2)} p^{2k-2} + G(q) + \bar{G}(\bar{q}) + \mathcal{O}(q), \quad (4.27)$$

where the coefficients in the sum over k come from an explicit expansion of the three-point classical action $S_3^{cl}(\frac{1}{4}, \frac{1}{4}, \frac{1}{4} + p^2)$. Differentiating this action with respect to p leads to the saddle point equation,

$$\begin{aligned} 0 &= \frac{\partial S_L^{cl}(q, \bar{q}; p)}{\partial p} \\ &= -2\pi + 16p \log 2 - 2p \log(q\bar{q}) + 16p^3 \sum_{k=1}^{\infty} \frac{(-1)^{k-1} (1-4^k) \zeta(2k+1)}{(2k+1)} p^{2k-2} + \mathcal{O}(q). \end{aligned} \quad (4.28)$$

Rewriting this equation in terms of the previously defined parameter $\varepsilon(q, \bar{q})$ leads to the relation,

$$\varepsilon(q, \bar{q}) = p + \frac{8}{\pi} \varepsilon(q, \bar{q}) p^3 \sum_{k=1}^{\infty} \frac{(-1)^{k-1} (1-4^k) \zeta(2k+1)}{(2k+1)} p^{2k-2} + \mathcal{O}(q), \quad (4.29)$$

which we can once again invert to solve for p_s as a power series in $\varepsilon(q, \bar{q})$ of the form (4.24). With this value of the saddle point momentum in hand, we can then compute the on-shell action $S_L^{cl}(q, \bar{q}; p)$ and the metric $g_{q\bar{q}}$ to an arbitrarily high order in $\varepsilon(q, \bar{q})$.

For example, the solution for the saddle point momentum up to $\mathcal{O}(\varepsilon^8)$ is

$$p_s(q, \bar{q}) = \varepsilon(q, \bar{q}) + \frac{8\zeta(3)}{\pi} \varepsilon(q, \bar{q})^4 - \frac{24\zeta(5)}{\pi} \varepsilon(q, \bar{q})^6 + \frac{192\zeta(3)^2}{\pi^2} \varepsilon(q, \bar{q})^7 + \mathcal{O}(\varepsilon^8). \quad (4.30)$$

This leads to the following values of the Liouville on-shell action,

$$S_L^{cl}(q, \bar{q}; p) = -\pi \varepsilon(q, \bar{q}) - 4\zeta(3) \varepsilon(q, \bar{q})^4 + 8\zeta(5) \varepsilon(q, \bar{q})^6 - \frac{64\zeta(3)^2}{\pi} \varepsilon(q, \bar{q})^7 + \mathcal{O}(\varepsilon^8), \quad (4.31)$$

and the Weil-Petersson metric,

$$g_{q\bar{q}} = \frac{8\pi^3}{q\bar{q}(\log \frac{2^8}{q\bar{q}})^3} \left[1 + \frac{40\pi^2 \zeta(3)}{(\log \frac{2^8}{q\bar{q}})^3} - \frac{168\pi^4 \zeta(5)}{(\log \frac{2^8}{q\bar{q}})^5} + \frac{1792\pi^4 \zeta(3)^2}{(\log \frac{2^8}{q\bar{q}})^6} + \dots \right], \quad (4.32)$$

at this order. Note that in this expansion the metric depends only on the norm $q\bar{q}$ and not on the phase of q . This is an artifact of our expansion at the perturbative level, and will no longer hold once non-perturbative corrections are included.

We plot the resulting expression for $g_{x\bar{x}}$ in the cross ratio coordinate in figure 3.

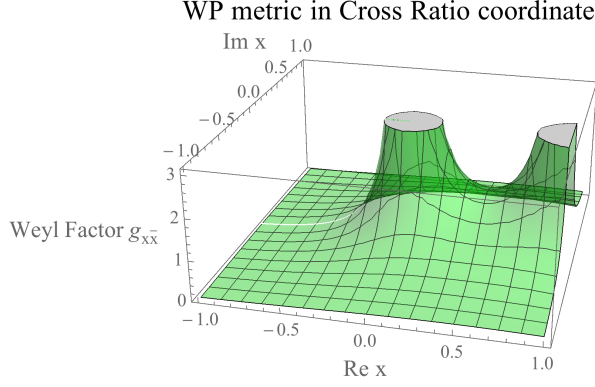


Figure 3: A plot of the Weil–Petersson metric on $\mathcal{M}_{0,4}$. We include up to $O((\log(q))^{50})$ terms.

4.3 Non-perturbative corrections to the metric

Having discussed the solution to the saddle-point equation and the computation of the Weil–Petersson metric at leading order in the q -expansion of the conformal block $f(p, x)$ in the previous section, we now outline a method to incorporate higher-order terms $f(p, x)$ in these quantities. We refer to these terms as non-perturbative corrections since a power series in q behaves like $\exp(-1/\varepsilon(q, \bar{q}))$.

We begin by writing the q -expansion of the semiclassical conformal block as,

$$\begin{aligned}
 f_{\frac{1}{4}+p^2} \left[\begin{array}{c} \frac{1}{4} \quad \frac{1}{4} \\ \frac{1}{4} \quad \frac{1}{4} \end{array} \right] (x) \\
 = -\frac{1}{4} \log x - \frac{1}{4} \log(1-x) - \frac{7}{4} \log \frac{2}{\pi} K(x) + p^2 \log 16 + p^2 \log q(x) + h_{\frac{1}{4}+p^2} \left[\begin{array}{c} \frac{1}{4} \quad \frac{1}{4} \\ \frac{1}{4} \quad \frac{1}{4} \end{array} \right] (q),
 \end{aligned} \tag{4.33}$$

where we introduce the function h which includes the contribution to $f(p, x)$ which appears as a power series in q (and which we dropped in our analysis in the previous section) and which has the expansion,

$$\begin{aligned}
 h_{\frac{1}{4}+p^2} \left[\begin{array}{c} \frac{1}{4} \quad \frac{1}{4} \\ \frac{1}{4} \quad \frac{1}{4} \end{array} \right] (q) &= \frac{1}{4(1+p^2)} q^2 \\
 &+ \left(\frac{-1}{32(1+p^2)^3} + \frac{3}{128(1+p^2)^2} + \frac{15}{128(1+p^2)} + \frac{81}{128(4+p^2)} \right) q^4 \\
 &+ \left(\frac{1}{96(1+p^2)^5} - \frac{5}{384(1+p^2)^4} - \frac{9}{256(1+p^2)^3} + \frac{56}{2048(1+p^2)^2} \right. \\
 &\left. + \frac{661}{16384(1+p^2)} - \frac{9}{128(4+p^2)} + \frac{16875}{16384(9+p^2)} \right) q^6 + \dots .
 \end{aligned} \tag{4.34}$$

We denote this function $h(p, q)$ for simplicity. These formulas derive simply from the recursion relations of Zamolodchikov [3].

Expanding $h(p, q)$ also as a power series in p , we can write

$$\begin{aligned} h(p, q) &= \frac{1}{4}q^2 + \frac{137}{512}q^4 + \frac{197}{1536}q^6 + \dots \\ &+ \left(-\frac{1}{4}q^2 - \frac{225}{2048}q^4 - \frac{5}{6144}q^6 + \dots \right) p^2 \\ &+ p^4 \sum_{k=1}^{\infty} A_k(q) p^{2k-2}, \end{aligned} \quad (4.35)$$

where $A_k(q)$ is a series of q obtained from the p expansion of the conformal blocks. Note that every series is expanded as $A_k(q) = a_k q^2 + \dots$. The first few $A_k(q)$ are

$$\begin{aligned} A_1(q) &= \frac{1}{4}q^2 + \frac{81}{8192}q^4 - \frac{12787}{221184}q^6 + \dots, \\ A_2(q) &= -\frac{1}{4}q^2 + \frac{3247}{32768}q^4 + \frac{732043}{7962624}q^6 + \dots. \end{aligned} \quad (4.36)$$

We also define the coefficients of the p^0 and p^2 terms in the expansion of $h(p, q)$ to be

$$A_{\text{indep}}(q) = \frac{1}{4}q^2 + \frac{137}{512}q^4 + \frac{197}{1536}q^6 + \dots \quad (4.37)$$

and

$$A_{\text{leading}}(q) = -\frac{1}{4}q^2 - \frac{225}{2048}q^4 - \frac{5}{6144}q^6 + \dots, \quad (4.38)$$

respectively. Using this notation, the p -expansion of the conformal block is given by,

$$h(p, q) = A_{\text{indep}}(q) + p^2 A_{\text{leading}}(q) + p^4 \sum_{k=1}^{\infty} A_k(q) p^{2k-2}, \quad (4.39)$$

where each coefficient is also a power series in q as described above.

Plugging in (4.2), we can now write the full Liouville action as

$$\begin{aligned} S_L^d(q, \bar{q}; p) &= G(q) + \bar{G}(\bar{q}) - 2\pi p + 8p^2 \log 2 - p^2 \log(q\bar{q}) - (A_{\text{leading}}(q) + A_{\text{leading}}(\bar{q}))p^2 \\ &+ 16p^4 \sum_{k=1}^{\infty} \frac{(-1)^{k-1}(1-4^k)\zeta(2k+1)}{(2k+1)(2k+2)} p^{2k-2} - p^4 \sum_{k=1}^{\infty} A_k(q) p^{2k-2} - p^4 \sum_{k=1}^{\infty} A_k(\bar{q}) p^{2k-2}, \end{aligned} \quad (4.40)$$

where we have absorbed the p independent piece $A_{\text{indep}}(q)$ into the pure gauge part $G(q)$. In the following we outline a procedure to solve the saddle-point equation and thus compute the metric after incorporating these additional corrections arising from the p -expansion of $h(p, q)$.

The expansion at leading order in p

Note that now in (4.40) the leading order piece in p contains contributions from the non-perturbative corrections $A_{\text{leading}}(q)$. The Liouville action up to order p^2 (and ignoring p independent terms) becomes

$$S_L^{cl}(q, \bar{q}; p) = -2\pi p + p^2 \left[\log \frac{2^8}{q\bar{q}} - (A_{\text{leading}}(q) + A_{\text{leading}}(\bar{q})) \right] + \mathcal{O}(p^4), \quad (4.41)$$

leading to the saddle point equation at order p :

$$\frac{\partial}{\partial p} S_L^{cl}(q, \bar{q}; p) = -2\pi p + 16p \log 2 - 2p \log(q\bar{q}) - 2p(A_{\text{leading}}(q) + A_{\text{leading}}(\bar{q})) = 0. \quad (4.42)$$

This equation determines the saddle point value $p_s(q)$ as

$$\begin{aligned} p_s(q) &= \frac{\pi}{\log \frac{2^8}{q\bar{q}} - A_{\text{leading}}(q) - A_{\text{leading}}(\bar{q})} \\ &= \frac{\pi}{\log \frac{2^8}{q\bar{q}} + \frac{1}{4}(q^2 + \bar{q}^2) + \frac{225}{2048}(q^4 + \bar{q}^4) + \frac{5}{6144}(q^6 + \bar{q}^6) + \dots}. \end{aligned} \quad (4.43)$$

Just as in the previous section, if we define a variable $\varepsilon(q, \bar{q})$ to be the leading-order (in p) value of the saddle point momentum, i.e.

$$\varepsilon(q, \bar{q}) := \frac{\pi}{\log \frac{2^8}{q\bar{q}} - A_{\text{leading}}(q) - A_{\text{leading}}(\bar{q})}, \quad (4.44)$$

we can write the Liouville on-shell action at this order as

$$S_L^{cl}(q, \bar{q}; p_s(q)) = -2\pi p_s(q) + \pi \frac{p_s(q)^2}{\varepsilon(q, \bar{q})} = -\pi \varepsilon(q, \bar{q}) \quad (4.45)$$

Therefore, just by redefining $\varepsilon(q, \bar{q})$ from its value in the previous section, we can represent both the saddle point equation and the Liouville action in the same manner.

Given this value of the classical action, we can compute the Weil-Petersson metric including corrections coming from the conformal block up to order q^2 (at this order p^2):

$$\boxed{g_{q\bar{q}} = 4\pi \partial_q \partial_{\bar{q}} \left(\frac{\pi^2}{\log(\frac{2^8}{q\bar{q}}) + \frac{1}{4}q^2 + \frac{1}{4}\bar{q}^2} + \dots \right) dq d\bar{q} = \frac{128\pi^3(2 - q^2)(2 - \bar{q}^2)}{q\bar{q}(4 \log(\frac{2^8}{q\bar{q}}) + q^2 + \bar{q}^2)^3} dq d\bar{q} + \dots} \quad (4.46)$$

Including subleading orders in p

Finally, we briefly summarize the method to compute the metric including subleading terms in the expansion of $h(p, q)$. We can express the full Liouville action (4.40) (omitting the p independent terms), including the newly-defined parameter $\varepsilon(q, \bar{q})$, as,

$$\begin{aligned} S_L^{cl}(q, \bar{q}; p) &= -2\pi p + \pi \frac{p}{\varepsilon(q, \bar{q})} \\ &+ 16p^4 \sum_{k=1}^{\infty} \frac{(-1)^{k-1} (1 - 4^k) \zeta(2k+1)}{(2k+1)(2k+2)} p^{2k-2} - p^4 \sum_{k=1}^{\infty} A_k(q) p^{2k-2} - p^4 \sum_{k=1}^{\infty} A_k(\bar{q}) p^{2k-2}, \end{aligned} \quad (4.47)$$

which leads to the full saddle point equation,

$$\begin{aligned} \frac{\partial}{\partial p} S_L^{cl}(q, \bar{q}; p) &= -2\pi + 2\pi \frac{p}{\varepsilon(q, \bar{q})} + 16p^3 \sum_{k=1}^{\infty} \frac{(-1)^{k-1} (1 - 4^k) \zeta(2k+1)}{2k+1} p^{2k-2} \\ &\quad - p^3 \sum_{k=1}^{\infty} (2k+2) A_k(q) p^{2k-2} - p^3 \sum_{k=1}^{\infty} (2k+2) A_k(\bar{q}) p^{2k-2} = 0, \end{aligned} \quad (4.48)$$

which we can again solve for p recursively in ε , by assuming a power series solution.

We forego explicitly solving this equation to any higher order than we have already discussed because—as we will see in a moment—the solutions for the metric at the orders we have described already reproduce certain geometric quantities to extremely high accuracy.

Before doing so, we note that there is one final way that the accuracy of our approximation can be improved: we can use the S^3 symmetries of moduli space described in equation (3.6). These are isometries of the WP metric. Our approximation for the metric is an expansion in cross-ratio, so will be most accurate when the cross ratio is small. In particular it is most accurate in the fundamental domain depicted in figure 2. To obtain the metric at an arbitrary point in moduli space we will use an S^3 symmetry to map the point into the fundamental domain, and only then use our approximate form of the metric. This is much more accurate than simply employing our approximation outside of the fundamental domain.

4.4 Comparison: the Weil–Petersson volume of $\mathcal{M}_{0,4}$

We will now check that the approximations described above are accurate.

We will begin by studying the volume of the moduli space $\text{Vol}(\mathcal{M}_{0,4})$ using our approximation for the metric $g_{q\bar{q}}$. In the case of the moduli space of the four punctured sphere, the exact Weil–Petersson volume is [35],

$$\text{Vol}(\mathcal{M}_{0,4}) = 2\pi^2. \quad (4.49)$$

Of course we can also compute the volume once we have $g_{q\bar{q}}$ on $\mathcal{M}_{0,4}$ by integrating the metric over the moduli space:

$$\text{Vol}(\mathcal{M}_{0,4}) = \int_{\mathcal{M}_{0,4}} g_{q\bar{q}} dq d\bar{q}. \quad (4.50)$$

We can therefore compare our expansion for $g_{q\bar{q}}$ from the previous sections to the exact result.

Furthermore, we can also test the accuracy of our result for the saddle point momentum $p_s(q)$ by computing the s -channel geodesic length at certain points in moduli space where the result is known exactly; in fact, this was already done in [13]. Recall the relationship between the saddle point momentum and the geodesic length, $\ell_s = 4\pi p_s$, discussed in §2.2. At certain values of the cross ratio x , the quantity $\cosh\left(\frac{\ell_s(x)}{2}\right)$ is known exactly, and thus we can also compare $\cosh(2\pi p_s)$ using our approximation of p_s to a given order.

In Table 1, we compare our approximation to the saddle point momentum p_s using the methods of §4.2 at two values of the cross ratio – $x = 1/2$ and $x = e^{i\frac{\pi}{3}}$ – to the exact

	$\cosh(2\pi p_s(1/2))$	$\cosh(2\pi p_s(e^{i\frac{\pi}{3}}))$	$g_{x\bar{x}}(1/2, 1/2)$	$g_{x\bar{x}}(e^{i\frac{\pi}{3}}, e^{-i\frac{\pi}{3}})$	$\text{Vol}(\mathcal{M}_{0,4})$
ε	2.74714	3.09768	1.23554	0.17457	17.5319
ε^4	3.00499	3.50136	1.58983	0.23704	19.701
ε^6	2.95594	3.41134	1.49928	0.218534	19.2835
ε^7	3.00215	3.5027	1.61307	0.243571	19.7552
ε^{18}	3.00082	3.50061	1.61307	0.243636	19.7455
ε^{60}	3.00039	3.49872	1.60833	0.242613	19.7374
Exact value	3	$\frac{7}{2}$			$2\pi^2$

Table 1: The value of s -channel geodesic length $\cosh(l_s/2) = \cosh(2\pi p_s(x))$ and the Weil-Petersson metric $g_{x\bar{x}}(x, \bar{x})$ in the cross ratio coordinate x using the perturbative expansion of the saddle point momentum outlined in §4.2, and at leading order in the expansion of $f(p, x)$. ε^k is the order of the $\varepsilon(q, \bar{q})$ expansion in p_s and the Liouville action $S_L(p_s(q), q)$. The final column lists our results for the volume of $\mathcal{M}_{0,4}$. The exact volume is $2\pi^2 \approx 19.7392$.

values. We also compute the value of the metric $g_{x\bar{x}}$ in the cross ratio coordinate at these points, as well as our approximation of $\text{Vol}(\mathcal{M}_{0,4})$ using our result for the metric. We show results for different orders in the perturbative expansion in $\varepsilon(q, \bar{q})$ of p_s , at leading order in the conformal block expansion of $f(p, x)$. Once we include corrections up to $\mathcal{O}(\varepsilon^{60})$, our approximate results differ from the exact values by about 10^{-3} .

	$\cosh(2\pi p_s(1/2))$	$\cosh(2\pi p_s(e^{i\frac{\pi}{3}}))$	$g_{x\bar{x}}(1/2, 1/2)$	$g_{x\bar{x}}(e^{i\frac{\pi}{3}}, e^{-i\frac{\pi}{3}})$	$\text{Vol}(\mathcal{M}_{0,4})$
ε	2.74714	3.09768	1.23554	0.17457	17.5319
ε^4	3.00458	3.50269	1.5868	0.238094	19.7028
ε^6	2.95555	3.41255	1.49643	0.219498	19.2851
ε^7	3.00174	3.50399	1.6101	0.244603	19.7570
ε^{18}	3.00042	3.501908	1.60752	0.244669	19.7445
ε^{60}	3.000000	3.500012	1.60537	0.243637	19.73922074
Exact value	3	$\frac{7}{2}$			$2\pi^2$

Table 2: The value of s -channel geodesic length $\cosh(l_s/2) = \cosh(2\pi p_s(x))$ and the Weil-Petersson metric $g_{x\bar{x}}(x, \bar{x})$ in the cross ratio coordinate x using the perturbative expansion of the saddle point momentum outlined in §4.3, including order q^2 non-perturbative corrections coming from the expansion of $f(p, x)$. ε^k is the order of the $\varepsilon(q, \bar{q})$ expansion in p_s and the Liouville action $S_L(p_s(q), q)$. The final column lists our results for the volume of $\mathcal{M}_{0,4}$. The exact volume is $2\pi^2 \approx 19.7392$.

In Table 2, we show the same results for geodesic lengths, the metric, and the volume of moduli space, now using the methods of §4.3. More specifically, we compute the solution of (4.48) up to order $(\varepsilon(q, \bar{q}))^{60}$ including order q^2 non-perturbative corrections arising from

the q -expansion of $f(p, x)$. We find that our results are extremely accurate even though we include just the first correction term in the expansion of the conformal block. For example, we find a difference in the approximate volume of $\mathcal{M}_{0,4}$ and the true value at order $(\varepsilon(q, \bar{q}))^{60}$ of

$$\frac{\text{Vol}(\mathcal{M}_{0,4})_{\text{approx}}}{2\pi^2} - 1 \approx 6.04777 \times 10^{-7}. \quad (4.51)$$

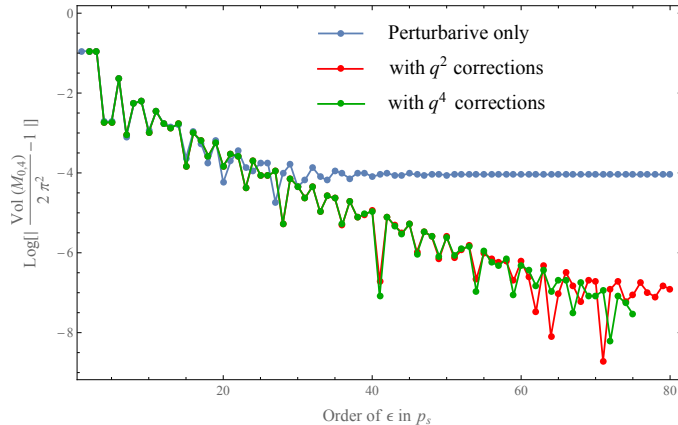


Figure 4: Plot of $|\frac{\text{Vol}(\mathcal{M}_{0,4})_{\text{approx}}}{2\pi^2} - 1|$ at each order of ε . Without non-perturbative corrections, the approximate volume converges around 19.7374 and the difference is $|\frac{\text{Vol}(\mathcal{M}_{0,4})_{\text{approx}}}{2\pi^2} - 1| \approx 9.1 \times 10^{-5}$. Including non-perturbative corrections of order q^2 , the difference continues to decrease after the perturbative results saturate.

Finally, in Figure 4 we plot the difference $|\frac{\text{Vol}(\mathcal{M}_{0,4})_{\text{approx}}}{2\pi^2} - 1|$ as a function of the order ε , both with and without the including the q^2 term in the expansion of the conformal block $f(p, x)$. We see a clear decrease when we increase the order of ε , which saturates at a particular value if we only include the perturbative corrections (leading order in $f(p, x)$), but continues to decrease substantially once we include the first nonzero term in the q -expansion of the conformal block. We expect this pattern to continue, and that as more terms in the perturbative and non-perturbative expansions are included our results will continue to improve.

5 The spectrum on moduli space

In this section, we study the spectrum of the Weil–Petersson Laplacian on the moduli space $\mathcal{M}_{0,4}$. This describes the quantum mechanics of a particle moving on the moduli space $\mathcal{M}_{0,4}$ with Hamiltonian equal to the Weil–Petersson Laplacian, and can be viewed as a simple theory of quantum geometry/quantum gravity. We thus study the equation

$$\Delta^{WP} \psi_n = E_n \psi_n, \quad (5.1)$$

where Δ^{WP} is the Laplacian constructed from the WP metric and ψ_n is the n th eigenfunction, with corresponding eigenvalue E_n .

In the rest of this section, we present our numerical results on the values and statistics of the E_n . We begin by briefly describing our method for numerically solving equation (5.1) in §5.1. For simplicity we will focus on the eigenfunctions which obey Dirichlet boundary conditions on the (half) fundamental domain depicted in Figure 2. This is equivalent to restricting to the sector which is invariant under the S_3 symmetry of $\mathcal{M}_{0,4}$ and anti-symmetric under complex conjugation in x .⁵ We will plot sample eigenfunctions ψ_n on the (half) fundamental domain. In appendix A, we present explicit numerical values computed using the method described in §5.1 in Tables 4 and 5. Then we move on to analyze the statistics of the spectrum. In §5.2 we verify that our results obey Weyl’s law, which describes the asymptotic eigenvalue density at large n . We next analyze the level statistics of the eigenvalues, computing the adjacent gap ratio (§5.3) and spectral form factor (§5.4). These are probes of the spacings of eigenvalues, and in both cases we find behavior characteristic of the Gaussian Orthogonal Ensemble (GOE) universality class. This is evidence that the quantum mechanical system described above has quantum chaotic behavior.

5.1 The spectrum of eigenvalues

Using the expansion in $\varepsilon \sim \log q$ and q we developed in §4, we can calculate the expansion of the metric analytically up to order $\mathcal{O}(q^m, (\log q)^n)$ for any desired values of m and n . We then proceed numerically by first discretizing the moduli space (with respect to the flat metric) such that the area of each element is less than some fixed value A_{UV} , and then numerically solving Laplace’s equation. A pictorial example of such a discretization is illustrated in Figure 5, though the actual sizes of A_{UV} used in our calculations are 10^{-4} or 10^{-5} , much smaller than that displayed in Figure 5.

We work on the half-fundamental domain in the τ coordinate, introduced in §3. We first compute the WP metric to very high accuracy using the rapidly convergent q -expansion of the conformal blocks, and then convert the result to a function of τ . In the q variable, there is a high concentration of volume of the moduli space near the cusp $q = 0$ (or correspondingly $x = 0$ in the cross-ratio coordinate), and this leads to higher errors in the numerical solution of (5.1). By numerically solving (5.1) after converting to the τ coordinate, where this cusp is mapped to $\tau = i\infty$, this problem is avoided and we are able to achieve stable results for the eigenvalues at lower orders in q .

As our goal is to analyze the statistics of the eigenvalue spectrum (rather than study the eigenvalues themselves), we find it convenient to make use of the following symmetries of the Laplacian. Firstly, the Weil–Petersson metric in the cross-ratio coordinate is invariant under the S_3 symmetry described in (3.6). Additionally, there is a \mathbb{Z}_2 symmetry under complex conjugation, which exchanges $x \leftrightarrow \bar{x}$. This is equivalent to $\tau \leftrightarrow -\bar{\tau}$. The S_3 and complex conjugation symmetries commute with one another, and also commute with the Laplacian. Thus when we solve Laplace’s equation we can restrict to the sector where the wavefunction is symmetric under S_3 and anti-symmetric under the complex conjugation

⁵The methods used in this section can easily be adapted to study more general classes of eigenfunctions as well.

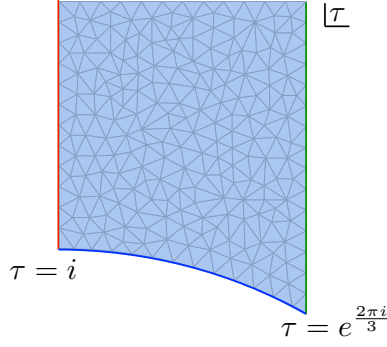


Figure 5: An example of the discretization of half-fundamental domain of the moduli $\mathcal{M}_{0,4}$. In this example, the area (with respect to the flat metric, not the WP metric) of each triangle is less than 0.001.

$\mathbb{Z}_2 := \{1, K\}$; i.e. the wavefunctions in this sector satisfy

$$g \cdot \psi(x) = \psi(g^{-1} \cdot x) = \psi(x), \quad \text{for } g \in S_3, \quad (5.2)$$

and

$$K \cdot \psi(x) = \psi(K \cdot x) = -\psi(x), \quad \text{for } K \in \mathbb{Z}_2. \quad (5.3)$$

This is equivalent to imposing Dirichlet boundary conditions on the boundary of the half-fundamental domain.

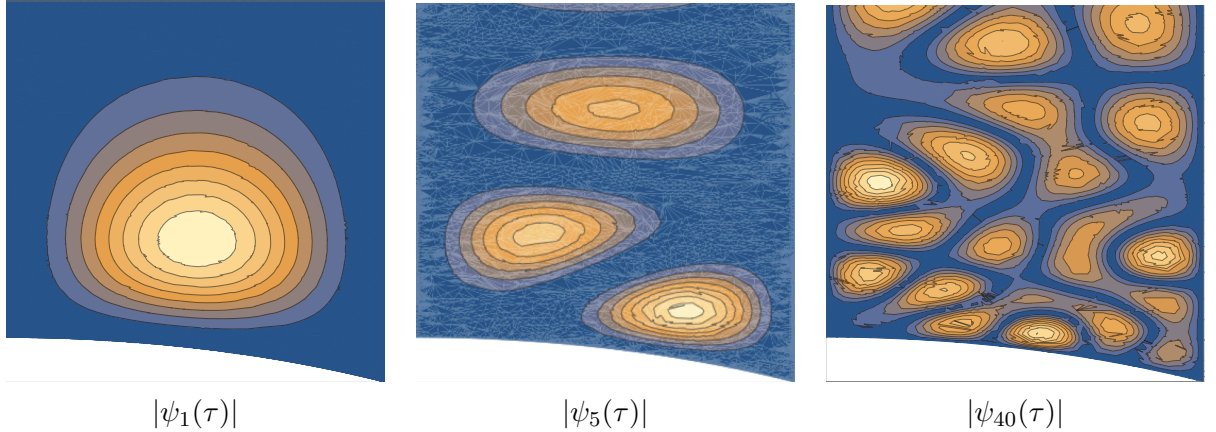


Figure 6: A contour plot of the absolute value of our numerical results for selected eigenfunctions of the Laplacian Δ^{WP} on the half fundamental domain in the τ coordinate. On the left is the ground state, $\psi_1(\tau)$, in the middle is the fifth excited state, $\psi_5(\tau)$, and on the right is the 40th excited state, $\psi_{40}(\tau)$. Note: these plots are cut off at a finite value of $\text{Im}(\tau)$.

When we numerically solve (5.1), we obtain both the eigenvalues and the corresponding eigenfunctions of Δ^{WP} . Though we are mainly interested in analyzing the statistics of

the eigenvalues in the following sections, it is also interesting to observe the form of the eigenfunctions we obtain. We plot a few examples in Figure 6.

5.2 Asymptotic density of the spectrum: Weyl's law

As a consistency check of our computation of the eigenvalues, we first verify Weyl's law, which describes the asymptotic density of the eigenvalues as a function of energy. More precisely, if we let $N(E)$ be the number of eigenvalues of the Laplacian of energy $\leq E$, then Weyl's law in two dimensions is given by (see, e.g., Ch. 16 of [36])

$$N(E) \approx \frac{A}{4\pi}E \mp \frac{L}{4\pi}\sqrt{E} + K, \quad (5.4)$$

where A is the area of the manifold on which we are computing the Laplacian, L is the length of the boundary and K is a constant which depends on the topology of the manifold, the shape of its boundary, and the boundary conditions one implements. Furthermore, the sign in front of the \sqrt{E} term depends on the boundary conditions: one has a positive or negative sign for Neumann or Dirichlet boundary conditions, respectively.

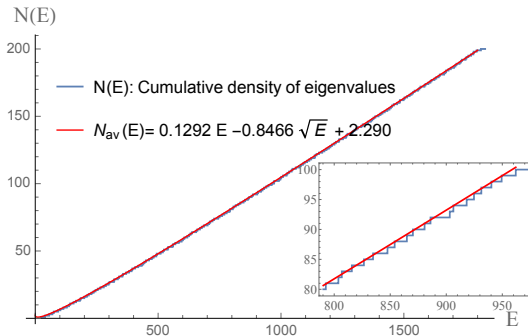


Figure 7: The plot of the number of eigenvalues $N(E)$ with eigenvalue $\leq E$. The blue line is the number of eigenvalues obtained numerically. The red line is the fit with the function (5.4). Weyl's law gives the first coefficient as $\pi/24 \approx 0.13$. To compute eigenvalues numerically, we truncate the expansion at q^0 (without non perturbative corrections) and $(\log q)^{-60}$. The inset is an expansion of the plot between 80th to 100th eigenvalues.

In Figure 7, we plot $N(E)$ for the first 200 numerically computed eigenvalues as a function of energy E , as well as the best fit of equation (5.4) to this distribution. Note that as we are solving Laplace's equation on a half-fundamental domain for the 6-fold symmetry group of moduli space, the expected coefficient of the linear term in E in Weyl's Law (5.4) is

$$\frac{A}{4\pi} = \frac{1}{4\pi} \times \frac{1}{2} \times \frac{2\pi^2}{6} = \frac{\pi}{24} \approx 0.13 .$$

The best fit of the curve plotted in Figure 7 has coefficient 0.1292, indicating strong agreement between our numerical results and Weyl's law.

5.3 Level statistics: Nearest neighbor correlations

In this section we begin our study of the level statistics of the spectrum. We start by analyzing the short-range correlations in the spectrum of eigenvalues, by studying the distribution of nearest neighbor level spacings.

To set the stage, we recall that for $N \times N$ Gaussian orthogonal matrices, the joint probability distribution for the eigenvalues E_i , $i = 1, \dots, N$, is given by ⁶

$$P_N(E_1, \dots, E_N) = C_N e^{-\frac{\beta}{4} \sum_{i=1}^N V(E_i)} \left(\prod_{1 \leq i, j \leq N} |E_i - E_j|^\beta \right), \quad (5.5)$$

with $V(E) = E^2$ and $\beta = 1$. The spectrum of the WP Laplacian will not exactly match this joint probability distribution. In particular, the quadratic potential $V(E)$ is specific to the Gaussian matrix ensemble. For a general chaotic system the form of the potential might be quite different. On the other hand, the Vandermonde determinant factor $\prod_{1 \leq i, j \leq N} |E_i - E_j|^\beta$ depends only on the symmetry class ($\beta = 1$ for GOE, $\beta = 2$ for GUE and $\beta = 4$ for GSE) of the problem, and not on the detailed form of the matrix potential. It describes a universal set of correlations between eigenvalues (essentially, eigenvalue repulsion) that is characteristic of any quantum chaotic system within that symmetry class. We will study this universal behaviour in the spectral statistics of the WP Laplacian.

Instead of working directly with the distribution of nearest neighbor spacings between eigenvalues, $s_n := E_{n+1} - E_n$, we work with the so-called adjacent gap ratio, r_n , defined by [38, 39],⁷

$$r_n := \frac{E_{n+1} - E_n}{E_n - E_{n-1}}, \quad (5.6)$$

where E_n is the n th energy eigenvalue of the system. Assuming our eigenvalues are drawn from an ensemble in RMT, the average of the adjacent gap ratio takes the form,

$$\langle r \rangle = \int_0^\infty r p(r) dr, \quad (5.7)$$

where $p(r)$ is the probability distribution of adjacent gap ratios. This quantity can be thought of as an analogue of Wigner’s surmise for the probability distribution of nearest neighbor spacings, $p(s)$, for spectra derived from random matrix ensembles [16]. Results for the probability densities $p(r)$ and average adjacent gap ratios $\langle r \rangle$ can be found in [39], and we reproduce them here in Table 3. The three RMT ensembles should be compared to Poisson statistics, the expected statistics of an integrable (non-chaotic) system. The smaller value of $\langle r \rangle$ with Poisson statistics reflects the absence of eigenvalue repulsion in an integrable system.

⁶For more complete reviews, see [16, 37] for example.

⁷Usually when one works directly with distribution of the nearest neighbor spacings s_n , one has to perform a process called “unfolding” the spectrum. In performing the unfolding, one essentially divides by the local density of the spectrum in order to achieve a mean level spacing of unity which can then be compared to results from RMT. A convenient feature of the adjacent gap ratio (5.6)—as described in [39]—is that we do not need to perform this unfolding of the spectrum, because the average density dependence cancels after taking the ratio of the level spacings.

	Poisson	GOE	GUE	GSE
$p(r)$	$\frac{1}{(1+r)^2}$	$\frac{27}{8} \frac{(r+r^2)}{(1+r+r^2)^{\frac{5}{2}}}$	$\frac{81\sqrt{3}}{4\pi} \frac{(r+r^2)^2}{(1+r+r^2)^4}$	$\frac{729}{4\pi} \frac{(r+r^2)^4}{(1+r+r^2)^7}$
$\langle r \rangle$	$2 \log 2 - 1 \approx 0.38629$	$4 - 2\sqrt{3} \approx 0.53590$	$2\frac{\sqrt{3}}{\pi} - \frac{1}{2} \approx 0.60266$	$\frac{32}{15}\frac{\sqrt{3}}{\pi} - \frac{1}{2} \approx 0.67617$

Table 3: Probability distribution $p(r)$ and average $\langle r \rangle$ of the adjacent gap ratio in systems whose eigenvalues obey either Poisson statistics, or statistics of one of the three ensembles from RMT [39].

The probability density of (5.6) diagnoses the random matrix behavior of a quantum system; it characterizes the short range correlation of energy levels because it depends on the nearest neighbor spacing of eigenvalues. By taking the expectation value of the parameter r , we can compare our results for the eigenvalues of the WP Laplacian on $\mathcal{M}_{0,4}$ to the results from RMT. In Figure 8, we compare both the probability distribution of the adjacent gap ratio $p(r)$ and the average $\langle r \rangle$ of our results to that of RMT. Our plots are based on the first 200 eigenvalues computed using an approximation of the WP metric up to $\mathcal{O}(q^0, (\log(q))^{-60})$.⁸

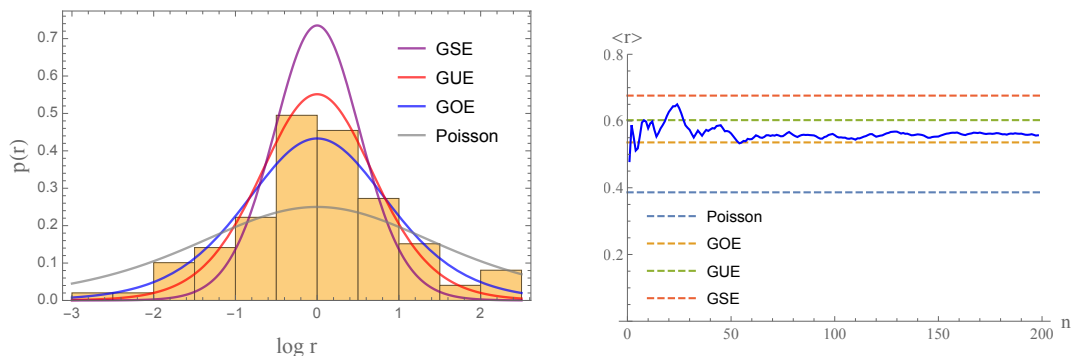


Figure 8: **Left:** Plot of the distribution of the adjacent gap ratio $\langle r_m \rangle$. The horizontal axis is the log of the gap ratio $\log r_m$ and the vertical axis is the eigenvalue density. These are binned by plotting the number of $\log r_m$ in $[x_0 + mr_0, x_0 + (m+1)r_0]$ divided by the total number M for $x_0 = 0$, $r_0 = 0.5$, $m \in \mathbb{Z}$ and $M = 200$. **Right:** Plot of the adjacent gap ratio $\langle r_n \rangle$. The vertical axis is the average of r_n from 1 to N levels: $\frac{1}{n} \sum_{n=1}^N r_n$. The horizontal axis is the level N up to which we average. These plots are computed using the numerical results for the first 200 eigenvalues arising from an approximation to the WP metric up to $\mathcal{O}(q^0, (\log(q))^{-60})$.

We note that the statistics of the eigenvalues of the WP Laplacian are far from Poisson; they clearly exhibit the eigenvalue repulsion characteristic of a chaotic system. Furthermore, we find that the closest ensemble is the GOE, which reflects the time reversal symmetry of the system. This is expected because we consider particle motion on the moduli

⁸The plots look essentially identical if we instead include the first 200 eigenvalues computed using an approximation to the WP metric with q^2 nonperturbative corrections.

space $\mathcal{M}_{0,4}$ without the presence of a time reversal symmetry breaking term such as an external magnetic field. More quantitatively, we compare the average of the r parameter. In the right plot in Figure 8, we show the average of the first n eigenvalues as a function of n , compared to the expected results from the ensembles presented in Table 3. As we take more eigenvalues, the expectation value $\langle r \rangle$ appears to approach that of the GOE. We take this as suggestive evidence that the spectral statistics for a particle moving on the moduli space $\mathcal{M}_{0,4}$, with Hamiltonian given by the WP Laplacian, is in the GOE universality class.

5.4 Level statistics: Spectral form factor

In this section we analyze the spectral form factor (SFF) of our system. This is a characterization of the two-point correlations in the eigenvalue spectrum $\langle \rho(E)\rho(E') \rangle$, and can be used to diagnose systems with quantum chaotic behavior. It is sensitive to long-range correlations between the eigenvalues of the system, and can also be used to demonstrate RMT behaviour.

The (SFF) $g(t; \beta)$ ⁹ is defined as the square of an analytically continued thermal partition function [40], which takes the form,

$$\begin{aligned} g(t; \beta) &:= |Z(\beta + it)|^2 = |\text{Tr}(e^{-\beta H} e^{-iHt})|^2 \\ &= \sum_{n,m} e^{-\beta(E_n + E_m)} e^{-i(E_n - E_m)t}, \end{aligned} \quad (5.8)$$

where H is the Hamiltonian of the system, β is the inverse temperature, and $t \geq 0$.

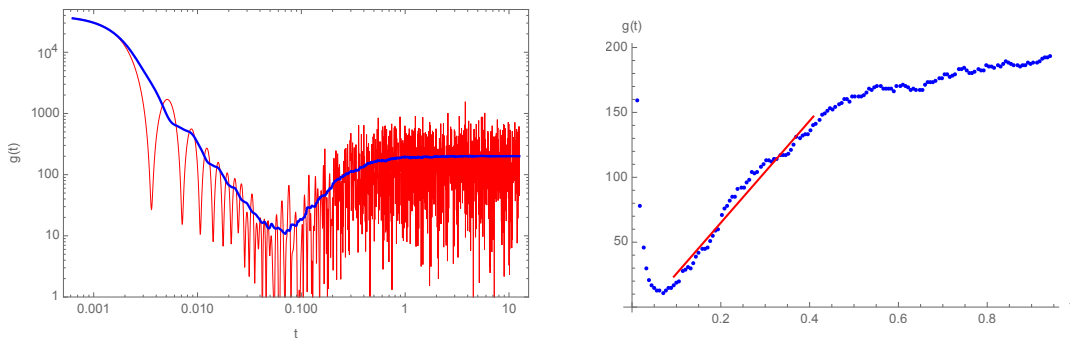


Figure 9: Left: The log-log plot of the spectral form factor. The blue line indicates the time average. **Right:** The plot of the spectral form factor (not on log scale). The red line is the linear fit of region $0.0942 < t < 0.408$.

The features of the spectral form factor for systems with random matrix behavior are as follows. Begin by separating the time t into four regimes, following [19]:

1. At early times t , the SFF decays exponentially in t . This behavior is often referred to as the slope.

⁹Strictly speaking, only the infinite temperature ($\beta = 0$) version of the analytically continued partition functions are referred to as spectral form factors in the quantum chaos literature, whereas a finite temperature extension is useful if we consider systems with infinite dimensional Hilbert spaces.

2. At some “dip time” t_d , the SFF reaches a minimum.
3. For $t_d < t < t_p$, the SFF increases linearly. This behavior is called the ramp.
4. Finally, at very late times, $t > t_p$ (the “plateau time”), the behavior crosses over to become a constant value. This region is referred to as the plateau.

The existence of the ramp characterizes the random matrix behavior of quantum systems. A linear ramp corresponds to long-distance level repulsion in the energy eigenvalues, with $\langle \rho(E)\rho(E') \rangle \propto \frac{1}{(E-E')^2}$. The early time decay is related to thermal relaxation and in dual theories of gravity is related to quasi-normal modes of black holes [19, 41]. The plateau at late times is a reflection of the discreteness of the spectrum. In particular, the long-time average of the spectral form factor approaches

$$\lim_{T \rightarrow \infty} \frac{1}{T} \int_0^T dt |Z(\beta + it)|^2 = \sum_n N_E e^{-2\beta E_n} \quad (5.9)$$

at late time, where N_E is the degeneracy in the number of states at energy E . If there are no degeneracies the late time value is given by the partition function $Z(2\beta)$.

The SFF of a chaotic theory typically exhibits erratic oscillations after the dip time, unless some sort of averaging is employed [42].¹⁰ Here we employ the time average [43]

$$g_{\text{t-ave}}(t; \beta) := \frac{1}{at} \int_{t-\frac{at}{2}}^{t+\frac{at}{2}} |Z(\beta + it)|^2 dt, \quad (5.10)$$

with $a = 1$. Note that the window over which we average grows linearly in time, so is a constant in the log-log plot.

The spectral form factors for the GOE, GUE and GSE ensembles of $N \times N$ matrices take the form [44],

$$\begin{aligned} |Z_{\text{GOE}}(it)|^2 &= Z_{\text{dip}}^2(t) + N \times \begin{cases} t - \frac{t}{2} \log(1+t) & t \leq 2 \\ 2 - \frac{t}{2} \log\left(\frac{t+1}{t-1}\right) & t > 2 \end{cases} \\ |Z_{\text{GUE}}(it)|^2 &= Z_{\text{dip}}^2(t) + N \times \begin{cases} \frac{t}{2} & t \leq 2 \\ 1 & t > 2 \end{cases} \\ |Z_{\text{GSE}}(it)|^2 &= Z_{\text{dip}}^2(t) + N \times \begin{cases} \frac{t}{4} - \frac{t}{8} \log\left|1 - \frac{t}{2}\right| & t \leq 4 \\ 1 & t > 4 \end{cases} \end{aligned} \quad (5.11)$$

where

$$Z_{\text{dip}}^2(t) = \frac{J_1(2Nt)^2}{t^2}, \quad (5.12)$$

and J_1 is the Bessel function of the first kind.

¹⁰For a Hamiltonian which is drawn from an ensemble (such as SYK) one can implement this averaging simply by averaging over draws from the ensemble. In the present case we have a single Hamiltonian so must employ a different type of averaging.

In this paper, we only study the spectrum of the symmetric sector of eigenfunctions, and thus our SFF is defined as,

$$g_{\text{sym}}(t; \beta) := |Z(\beta + it)|^2 = |\text{Tr}(P_{\text{sym}} e^{-\beta H} e^{-iHt})|^2, \quad (5.13)$$

where P_{sym} is the projection onto the symmetric sector defined by (5.2) and (5.3). Furthermore, we can only compute a finite number of eigenvalues in the spectrum numerically, so we truncate the sum over the spectrum as,

$$g_{\text{sym}}^{\text{truncate-}N}(t; \beta) := \sum_{i,j=1}^N e^{-\beta(E_i+E_j)} e^{-i(E_i-E_j)t}. \quad (5.14)$$

Here i, j label the spectrum of eigenvalues in the symmetric sector. In Figure 9, we plot the result for the SFF $g_{\text{sym}}^{\text{truncate-}200}(t; \beta)$ using the first 200 numerically-computed symmetric sector eigenvalues. Even though we truncate to only 200 eigenvalues, we are nevertheless clearly able to see a ramp characteristic of long distance eigenvalue repulsion. The ramp region is well fit by a linear function. This is further evidence that two-point statistics of eigenvalues exhibits features characteristic of quantum chaos.

Acknowledgements

We thank J. Chandra, S. Collier, K. Colville, T. Hartman, K. Namjou, S. Shenker, and H. Verlinde for helpful conversations. The work of S.M.H. is supported by the National Science and Engineering Council of Canada and the Canada Research Chairs program. Research of AM is supported in part by the Simons Foundation Grant No. 385602 and the Natural Sciences and Engineering Research Council of Canada (NSERC), funding reference number SAPIN/00047-2020. TN is supported by MEXT KAKENHI Grant-in-Aid for Transformative Research Areas A “Extreme Universe” Grant Number 22H05248.

A Numerical results for the eigenvalues

A.1 Numerical Data

In this section, we present the numerical data for the eigenvalues of the Laplacian on the moduli space $\mathcal{M}_{0,4}$. As discussed in the main text, for simplicity we consider only the eigenfunctions that obey (5.2) and (5.3). The results are shown in tables 4 and 5. Our methods can easily be adapted to compute the spectrum up to arbitrarily high energy levels.

A.2 On the accuracy of the eigenvalues

We now estimate the errors on eigenvalues that we numerically compute. These will depend on both the expansion in the coordinate q and the mesh size ΔA used when we discretize moduli space.

First we consider the finite ΔA effects. We are studying the eigenvalue problem defined by,

$$e^{-2\phi(x_1, x_2)} (\partial_{x_1}^2 + \partial_{x_2}^2) \psi(x_1, x_2) = E_n \psi(x_1, x_2), \quad (\text{A.1})$$

24.004	39.8792	56.4147	69.6923	75.6385	92.8046	102.244	114.388
128.198	137.274	142.367	155.89	166.06	181.288	185.131	199.328
209.627	217.81	228.69	237.372	245.334	254.32	265.377	278.709
287.302	298.239	302.096	320.042	321.723	335.921	341.145	354.566
357.093	369.811	381.324	391.954	395.11	406.473	418.95	433.165
439.53	444.306	450.738	462.997	474.166	481.323	492.444	494.414
509.797	519.197	523.611	538.689	541.022	558.767	560.818	570.013
584.012	595.434	600.936	606.644	618.73	625.725	631.78	638.204
654.643	659.605	670.042	677.64	686.185	701.319	707.672	712.033
721.206	727.92	744.16	750.174	760.372	769.299	778.799	790.252
792.521	803.731	806.792	815.748	826.515	834.676	847.554	853.963
864.855	870.227	880.657	885.938	903.13	906.36	918.201	924.741

Table 4: First 96 eigenvalues of the Laplacian on $\mathcal{M}_{0,4}$ at order $\mathcal{O}(q^0, (\log(q))^{65})$ (leading order in the conformal block expansion). The area of each discrete triangle in the fundamental domain with respect to the flat metric is taken to be smaller than 10^{-5} .

24.0024	39.8759	56.4075	69.6792	75.6396	92.7882	102.233	114.381
128.155	137.265	142.374	155.857	166.042	181.265	185.093	199.308
209.633	217.727	228.651	237.369	245.359	254.249	265.327	278.66
287.275	298.21	302.043	320.044	321.644	335.852	341.113	354.564
357.033	369.773	381.301	391.801	395.131	406.401	418.892	433.118
439.428	444.291	450.719	462.908	474.116	481.308	492.347	494.366
509.72	519.182	523.601	538.573	540.922	558.692	560.758	569.982
583.947	595.34	600.838	606.606	618.659	625.728	631.74	638.133
654.622	659.505	670.045	677.442	686.093	701.272	707.663	711.971
721.259	727.768	743.975	750.081	760.377	769.144	778.855	790.136
792.511	803.755	806.626	815.756	826.47	834.588	847.531	853.984
864.801	870.031	880.593	885.793	903.137	906.308	918.223	924.752

Table 5: First 100 eigenvalues of the Laplacian on $\mathcal{M}_{0,4}$ at order $\mathcal{O}(q^2, (\log(q))^{30})$ (including $O(q^2)$ corrections in the conformal block expansion). The area of each discrete triangle in the fundamental domain with respect to the flat metric is taken to be smaller than 10^{-4} .

where $x_1 = \text{Im}\tau$ and $x_2 = \text{Re}\tau$. Because the lattice spacing is given by $\sqrt{\Delta A}$, we estimate that the cut off of the “momentum” ∂_{x_i} is given by $1/\sqrt{\Delta A}$. To get a tighter bound, we replace $e^{2\phi(x_1, x_2)}$ by $\max(e^{2\phi(x_1, x_2)})$. Then, we expect that the cutoff of the energy is

$$E_n \leq \frac{1}{\max(e^{2\phi(x_1, x_2)})} \frac{1}{\Delta A}. \quad (\text{A.2})$$

Using Weyl’s law $N(E) \approx \frac{A}{4\pi} E$, we can trust the numerical results for eigenvalues which

satisfy

$$N(E) \ll \frac{1}{4\pi} \frac{1}{\max(e^{2\phi(x_1, x_2)})} \frac{A}{\Delta A}. \quad (\text{A.3})$$

For the sector of eigenfunctions we study on $\mathcal{M}_{0,4}$, $\max(e^{2\phi(x_1, x_2)}) = e^{2\phi(\frac{1}{2}, \frac{\sqrt{3}}{2})} \approx 0.8$ and $\frac{A}{4\pi} = 0.13$. Therefore, for example, when $\Delta A = 10^{-4}$, the bound on the eigenvalue is

$$N(E) \ll 1600. \quad (\text{A.4})$$

To visualize how the spectrum are stable under the change of mesh size or non-perturbative corrections, we show the shifts of eigenvalues in figure 10.

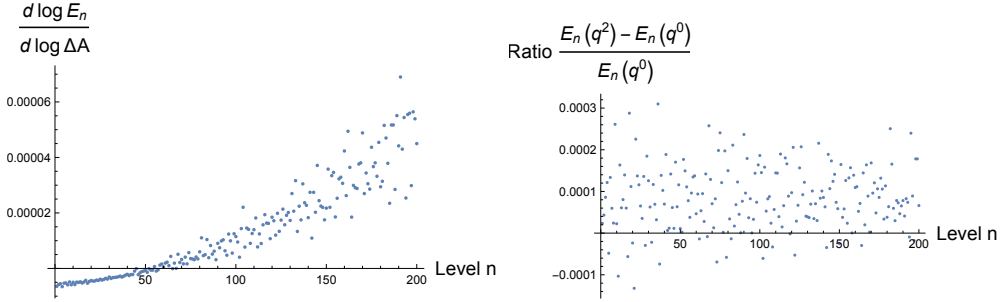


Figure 10: Left: The plot of $\frac{d \log E_n}{d \log \Delta A}$ for each eigenvalues E_n for $n = 1 \sim 200$ when the area ΔA of each mesh is smaller than 10^{-5} . To numerically calculate, we change the mesh size from 5.0×10^{-5} to 1.0×10^{-5} and use the approximate $\frac{d \log E_n}{d \log \Delta A}$ by the ratio of differences. **Right:** The shifts of eigenvalues when we include the $\mathcal{O}(q^2)$ corrections to the metric. $E_n(q^2)$ means the n -th eigenvalue at the order $\mathcal{O}(q^2, (\log |q|)^{-30})$ whereas $E_n(q^0)$ is that at the order $\mathcal{O}(q^0, (\log |q|)^{-30})$.

Next, we consider the effect of the finite truncation at $\mathcal{O}((\log |q|)^{-n}, q^m)$. As n is increased, the new subleading terms in $g_{q\bar{q}}$ are suppressed by powers of $\left(\log \frac{2^8}{q\bar{q}}\right)^{-1}$, which is quite small in the fundamental domain for x . For example at $x = \frac{1}{2}$ (on the boundary of the fundamental domain, where the errors will be the largest) we have $\left(\log \frac{2^8}{q\bar{q}}\right)^{-1} \approx 0.08$. Similarly, as m is increased subleading terms will be introduced which are suppressed by powers of q^2 , which at $x = \frac{1}{2}$ is $q^2 \approx 0.002$. This explains the results in Figure 4, where we see roughly 20-30 terms in the perturbative expansion (i.e. expansion in n) are needed before the non-perturbative expansion (the expansion in m) becomes important. It would be interesting to investigate the size of the error terms more quantitatively, which would require a study of the growth of the numerical coefficients which appear in this expansion; this may be possible using the Zamolodchikov recursion relations, but we will leave this for future work. It is, however, possible to check explicitly that the numerical results for the eigenvalues change only by small amounts as subleading terms are introduced; this is clear by comparing tables in A.1. In particular, by introducing an additional non-perturbative term in our approximation, the values of the eigenvalues only change by roughly one part in 10^{-4} .

References

- [1] A.M. Polyakov, *Quantum Geometry of Bosonic Strings*, *Phys. Lett. B* **103** (1981) 207.
- [2] A.B. Zamolodchikov, *CONFORMAL SYMMETRY IN TWO-DIMENSIONS: AN EXPLICIT RECURRENCE FORMULA FOR THE CONFORMAL PARTIAL WAVE AMPLITUDE*, *Commun. Math. Phys.* **96** (1984) 419.
- [3] A.B. Zamolodchikov, *Conformal symmetry in two-dimensional space: recursion representation of conformal block*, *Theoretical and Mathematical Physics* **73** (1987) 1088.
- [4] L.A. Takhtajan, *Liouville theory: Quantum geometry of Riemann surfaces*, *Mod. Phys. Lett. A* **8** (1993) 3529 [[hep-th/9308125](#)].
- [5] M. Matone, *Uniformization theory and 2-D gravity. 1. Liouville action and intersection numbers*, *Int. J. Mod. Phys. A* **10** (1995) 289 [[hep-th/9306150](#)].
- [6] L.A. Takhtajan, *Topics in quantum geometry of Riemann surfaces: Two-dimensional quantum gravity*, [hep-th/9409088](#).
- [7] H. Dorn and H.J. Otto, *Two and three point functions in Liouville theory*, *Nucl. Phys. B* **429** (1994) 375 [[hep-th/9403141](#)].
- [8] A.B. Zamolodchikov and A.B. Zamolodchikov, *Structure constants and conformal bootstrap in Liouville field theory*, *Nucl. Phys. B* **477** (1996) 577 [[hep-th/9506136](#)].
- [9] B. Ponsot and J. Teschner, *Liouville bootstrap via harmonic analysis on a noncompact quantum group*, [hep-th/9911110](#).
- [10] B. Ponsot and J. Teschner, *Clebsch-Gordan and Racah-Wigner coefficients for a continuous series of representations of $U(q)(sl(2,R))$* , *Commun. Math. Phys.* **224** (2001) 613 [[math/0007097](#)].
- [11] J. Teschner, *Liouville theory revisited*, *Class. Quant. Grav.* **18** (2001) R153 [[hep-th/0104158](#)].
- [12] J. Teschner, *From Liouville theory to the quantum geometry of Riemann surfaces*, in *Mathematical physics. Proceedings, 14th International Congress, ICMP 2003, Lisbon, Portugal, July 28-August 2, 2003*, 2003 [[hep-th/0308031](#)].
- [13] L. Hadasz, Z. Jaskolski and M. Piatek, *Classical geometry from the quantum Liouville theory*, *Nucl. Phys. B* **724** (2005) 529 [[hep-th/0504204](#)].
- [14] A. Eskin and M. Mirzakhani, *Counting closed geodesics in Moduli space*, *arXiv e-prints* (2008) arXiv:0811.2362 [[0811.2362](#)].
- [15] Z. Rudnick, *Goe statistics on the moduli space of surfaces of large genus*, 2022.
- [16] M. Mehta, *Random Matrices*, Academic Press (1991).
- [17] O. Bohigas, M.J. Giannoni and C. Schmit, *Characterization of chaotic quantum spectra and universality of level fluctuation laws*, *Phys. Rev. Lett.* **52** (1984) 1.
- [18] Bohigas, O., Giannoni, M.J. and Schmit, C., *Spectral properties of the laplacian and random matrix theories*, *J. Physique Lett.* **45** (1984) 1015.
- [19] J.S. Cotler, G. Gur-Ari, M. Hanada, J. Polchinski, P. Saad, S.H. Shenker et al., *Black Holes and Random Matrices*, *JHEP* **05** (2017) 118 [[1611.04650](#)].
- [20] N. Afkhami-Jeddi, A. Ashmore and C. Cordova, *Calabi-Yau CFTs and random matrices*, *JHEP* **02** (2022) 021 [[2107.11461](#)].

- [21] H.L. Verlinde, *Conformal Field Theory, 2-D Quantum Gravity and Quantization of Teichmuller Space*, *Nucl. Phys.* **B337** (1990) 652.
- [22] C. Scarinci and K. Krasnov, *The universal phase space of AdS₃ gravity*, *Commun. Math. Phys.* **322** (2013) 167 [[1111.6507](#)].
- [23] J. Kim and M. Porrati, *On a Canonical Quantization of 3D Anti de Sitter Pure Gravity*, *JHEP* **10** (2015) 096 [[1508.03638](#)].
- [24] A. Maloney, *Geometric Microstates for the Three Dimensional Black Hole?*, [1508.04079](#).
- [25] L. Eberhardt, *Off-shell Partition Functions in 3d Gravity*, [2204.09789](#).
- [26] W. Li, W. Song and A. Strominger, *Chiral Gravity in Three Dimensions*, *JHEP* **04** (2008) 082 [[0801.4566](#)].
- [27] P. Saad, S.H. Shenker and D. Stanford, *JT gravity as a matrix integral*, [1903.11115](#).
- [28] N. Seiberg, *Notes on quantum Liouville theory and quantum gravity*, *Prog. Theor. Phys. Suppl.* **102** (1990) 319.
- [29] Y. Nakayama, *Liouville field theory: A Decade after the revolution*, *Int. J. Mod. Phys. A* **19** (2004) 2771 [[hep-th/0402009](#)].
- [30] D. Harlow, J. Maltz and E. Witten, *Analytic Continuation of Liouville Theory*, *JHEP* **12** (2011) 071 [[1108.4417](#)].
- [31] A.B. Zamolodchikov, *Two-dimensional conformal symmetry and critical four-spin correlation functions in the Ashkin-Teller model*, *Sov. Phys. - JETP* **63** (1986) 1061.
- [32] M. Beşken, S. Datta and P. Kraus, *Semi-classical Virasoro blocks: proof of exponentiation*, *JHEP* **01** (2020) 109 [[1910.04169](#)].
- [33] P.G. Zograf and L.A. Takhtadzhyan, *On liouville's equation, accessory parameters, and the geometry of teichmüller space for riemann surfaces of genus 0*, *Matematicheskii Sbornik* **174** (1987) 147.
- [34] S.A. Wolpert, *Asymptotics of the spectrum and the selberg zeta function on the space of riemann surfaces*, *Comm. Math. Phys.* **108** (1987) 283.
- [35] S. Wolpert, *On the homology of the moduli space of stable curves*, *Annals of Mathematics* **118** (1983) 491.
- [36] M.C. Gutzwiller, *Chaos in classical and quantum mechanics*, Springer (1990).
- [37] T. Guhr, A. Muller-Groeling and H.A. Weidenmuller, *Random matrix theories in quantum physics: Common concepts*, *Phys. Rept.* **299** (1998) 189 [[cond-mat/9707301](#)].
- [38] Y.-Z. You, A.W.W. Ludwig and C. Xu, *Sachdev-ye-kitaev model and thermalization on the boundary of many-body localized fermionic symmetry-protected topological states*, *Phys. Rev. B* **95** (2017) 115150.
- [39] Y.Y. Atas, E. Bogomolny, O. Giraud and G. Roux, *Distribution of the Ratio of Consecutive Level Spacings in Random Matrix Ensembles*, *Physical Review Letters* **110** (2013) 084101 [[1212.5611](#)].
- [40] F. Haake, *Quantum Signatures of Chaos*, Springer Berlin Heidelberg (2010).
- [41] G.T. Horowitz and V.E. Hubeny, *Quasinormal modes of AdS black holes and the approach to thermal equilibrium*, *Phys. Rev. D* **62** (2000) 024027 [[hep-th/9909056](#)].

- [42] R.E. Prange, *The Spectral Form Factor Is Not Self-Averaging*, *Phys. Rev. Lett* **78** (1997) 2280 [[chao-dyn/9606010](#)].
- [43] V. Balasubramanian, B. Craps, B. Czech and G. Sárosi, *Echoes of chaos from string theory black holes*, *JHEP* **03** (2017) 154 [[1612.04334](#)].
- [44] J. Liu, *Spectral form factors and late time quantum chaos*, *Phys. Rev. D* **98** (2018) 086026 [[1806.05316](#)].